GMFβ CONTROLS BRANCHED ACTIN CONTENT AND LAMELLIPODIAL RETRACTION IN FIBROBLASTS

Elizabeth M. Haynes

A dissertation submitted to the faculty of the University of North Carolina at Chapel Hill in partial fulfillment of the requirements for the degree of Doctor of Philosophy in the Department of Cell Biology and Physiology in the College of Medicine.

Chapel Hill
2015

Approved by:

James Bear

Richard Cheney

Stephanie Gupton

Christopher Mack

Stephen Rogers

ABSTRACT

Elizabeth M. Haynes: GMFβ controls branched actin content and lamellipodial retraction in fibroblasts
(Under the direction of James E. Bear)

The lamellipodium is an important structure for cell migration containing branched actin nucleated via the Arp2/3 complex. The formation of branched actin is relatively well studied, but less is known about its disassembly and how this influences migration. GMF is implicated in both Arp2/3 debranching and inhibition of Arp2/3 activation. Modulation of GMFβ, a ubiquitous GMF isoform, by depletion or overexpression resulted in changes in lamellipodial dynamics, branched actin content and migration. Acute pharmacological inhibition of Arp2/3 by CK-666, coupled to quantitative live-cell imaging of the complex, showed depletion of GMFβ decreased the rate of branched actin disassembly. These data, along with mutagenesis studies, suggest that debranching (not inhibition of Arp2/3 activation) is a primary activity of GMFβ in vivo. Furthermore, depletion or overexpression of GMFβ disrupted the ability of cells to directionally migrate to a gradient of fibronectin (haptotaxis). These data suggest that debranching by GMFβ plays an important role in branched actin regulation, lamellipodial dynamics, and directional migration.

This work is dedicated to my parents and my grandmother. I couldn't ask for anyone more supportive and loving in my life.

In memory of my grandfather, who taught me the beauty and peace of nature from a young age.

ACKNOWLEDGEMENTS

The completion of this work has been a tremendous journey for me, and provided me the platform to grow both scientifically and personally. I have made deep friendships enforced by evenings of talking science and life. I have had the blessing of a lab equally eager to celebrate good data and troubleshoot bad data. To be surrounded by people who share in your awe as you observe the tiny wonders of life through a microscope eyepiece.

My committee also shares this outlook. Their enthusiasm and strong guidance through my project has helped me learn how to productively edit my ideas and communicate them more clearly.

Dr. Richard Cheney, thank you for your bottomless enthusiasm and insightful questions. I am envious of your memory of details, and truly loved rotating in your lab and getting my introduction to TIRF.

Dr. Stephanie Gupton, you have always been practical and on-point with your advice. It has been inspirational to watch you set up your lab and start getting papers out and receiving grants as a relatively new PI.

Dr. Steve Rogers, thank you for providing me a glimpse into working with a model organism and the charm of drosophila (especially Curly-Os). Again, rotating in your lab taught me so much… and not just from the hours of podcasts I burned through while working on imaging 96 well plates!

Dr. Chris Mack, I definitely owe my pre-doctoral fellowship to your support. That was such a huge contribution to my future as a scientist and the security of our lab.

Last but definitely not least, JBear! You have always been endlessly supportive of me, even when that meant letting me make my own mistakes in my experiments. You recognize when someone needs to prove a point for themselves, and the freedom you've given me to develop and explore ideas has been so valuable. You are not just a mentor, but a friend and a person I deeply respect. I hope one day to develop instincts as keen as yours for what science to pursue. The way you look at science and think about science will always influence my future work. You have definitely taught me the importance of questioning dogma, looking at the big picture, and appreciating the beauty of simple questions. I look forward to sharing a beer with you at conferences in the future and talking shop about microscopy techniques.

To my friends and colleagues in the lab, I would have to write a second thesis just to talk about how much I appreciate you all. I would especially like to thank Sam, Sreeja, Irina, Hailey, and Jeremy for ample scientific advice, empathy, and encouragement.

To my other science friends, especially Cortney, Kathryn, and Matt: you have all enriched my life and helped me improve as a person and scientist. And also for just letting me goof off and be myself with you.

Demi, you've been there for nearly my entire development as a scientist. Thank you for all the sharp wisdom, laughter, and 'burgin'.

Austin, you are by far the kindest person I have ever met. You have given me comfort and been my cheering section for the most intense times in my scientific career. Thank you for everything you do, including remembering the names of the proteins I work on.

PREFACE

Chapter 2 is a manuscript accepted in the Journal of Cell Biology. I performed all the experiments and drafted all the figures with input from Dr. James Bear. Dr. Sreeja Asokan, Dr. Samantha King, and Irina Lebedeva provided assistance making chemotaxis and haptotaxis chambers. Dr. Heath Johnson wrote the MatLab script analyzing the percentage of cell edge positive for Arp2/3. Dr. Jeremy Simon performed RNAseq analysis from data I generated, originally for a manuscript published in The Journal of Cell Biology (Wu et al., 2013). Dr. Congying Wu generated the Arp2/3 double knockdown cells (Wu and Asokan et al., Cell 2012).

TABLE OF CONTENTS

LIST OF FIGURES

LIST OF ABBREVIATIONS AND SYMBOLS

ADF	Actin Depolymerizing Factor
ADP	Adenosine Diphosphate
Arp	Actin Related Protein
ATP	Adenosine Triphosphate
BSA	Bovine Serum Albumin
Cdc42	Cell Division Control Protein 42
CNTL	Control
DMEM	Dulbecco's Modified Eagle Medium
ECM	Extracellular Matrix
GFP	Green Fluorescent Protein
GMF	Glia Maturation Factor
hr	Hour
IF	Immunofluorescence
JMY	Junction-Mediating and Regulatory Protein
KD	Knockdown
KDR	Knockdown-rescue
min	minute

NA	Numerical Aperture
NGS	Normal Goat Serum
NPF	Nucleation Promoting Factor
NS	Non-specific
PBS	Phosphate Buffered Saline
PDGF	Platelet Derived Growth Factor
RNA-seq	Ribonucleic acid sequencing
RPKM	Reads Per Kilobase Per Million Mapped Reads
s	second
SCAR/WAVE	Suppressor of Cyclic Adenosine Monophosphate Receptor/WASP-family Verprolin Homology Protein
shRNA	Short Hairpin Ribonucleic Acid
SSH1L	Slingshot Homology 1L
TagRFP-T	Tag Red Fluorescent Protein-T
WASH	WASP and SCAR homolog
WASP	Wiskott-Aldrich Syndrome Protein
WCA	WH2, Central Connector, Acidic Domain
WH2	WASP Homology 2
WHAMM	WASP Homolog associated with Actin, Membranes, and Microtubules

CHAPTER ONE: INTRODUCTION

Cell migration

From development onward, the process of cell migration is crucial to life. Migration of various cell types is necessary to complete embryogenesis and neural development (Lambrechts et al., 2004; Aman and Piotrowski, 2010). When an organism is wounded, cells must migrate to close that wound. In the case of an infection, leukocytes must be able to migrate to inflamed tissue and follow any invading pathogens (Wickramarachchi et al., 2010).

Cell migration can be subdivided into two morphologically distinct modes: mesenchymal and amoeboid migration (Lämmermann and Sixt, 2009; Lambrechts et al., 2004). In amoeboid migration, cells move rapidly and frequently extend and retract protrusions known as "pseudopods". Mesenchymal cells move more slowly and are led by a thin, fan shaped protrusion called the lamellipodium and by long finger-like structures known as filopodia. These structures are governed by cycles of protrusion, adhesion, and retraction, which when coupled to retraction in the rear of the cell, leads to net forward migration.

Directional Migration

The ability to migrate, however, is not the only requirement for development and maintenance of an organism. Cells must detect and respond appropriately to physiological

cues for the context of their migration. This is called *directional migration*. Both failure to migrate and failure to follow directional cues can cause migration defects, which can result in disease (Lambrechts et al., 2004).

Cells are capable of migrating in response to a diverse collection of cues, ranging from growth factors to substrate stiffness to electrical fields (Bear and Haugh, 2014). The most widely studied form of directional migration is chemotaxis, although most studies have been on amoeboid and not mesenchymal cells (Asokan et al., 2014; Bear and Haugh, 2014). Chemotaxis is defined as migration to a gradient of soluble chemical cues, such as growth factors or cytokines (Fig 1.1, left). Migration to surface bound cues is known as haptotaxis, and only recently have efforts to understand the requirements of haptotaxis begun in earnest (Fig 1.1, right) (Wu et al., 2012).

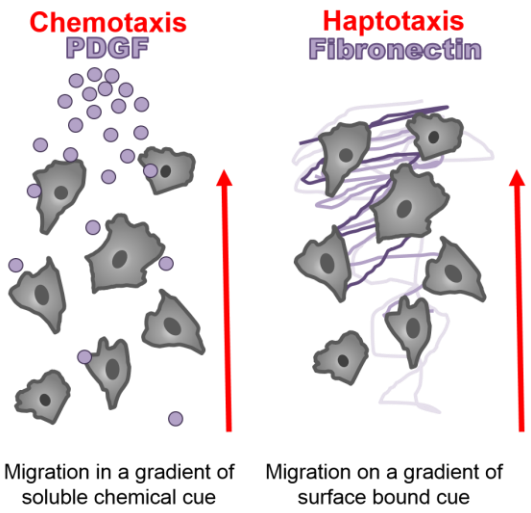

Figure 1.1 Two major forms of directed migration are chemotaxis and haptotaxis.

Chemotaxis is a form of directional migration where cells sense and migrate in response to soluble cues, often growth factors or cytokines. Haptotaxis is a form of directional migration where cells sense and migrate in response to a surface bound cue. This usually represents extracellular matrix proteins like fibronectin or collagen, but a hybrid form of chemotaxis and haptotaxis can be achieved by binding chemotactic proteins in a gradient to a glass surface. It is unknown whether this form of "haptotaxis" follows a haptotactic or chemotactic pathway.

Actin Polymerization and the Cytoskeleton

An important part of mesenchymal migration is the polymerization of a protein subunit called actin, into filaments. The polymerization of these filaments against the plasma membrane provides the mechanical force necessary to extend the leading edge of the cell, while myosin controls retraction of the rear of the cell. As the cell moves it produces nascent adhesions at the lamellipodial edge, which mature into focal adhesions. Focal adhesions provide a link between the substrate on which the cell is migrating (the extracellular matrix or ECM) and the cell body through thick F-actin cables called stress fibers.

Actin polymerization first requires that three globular (G) actin subunits come together in a process known as filament nucleation. Once an actin nucleus is formed, ATP-G-actin subunits are added on the fast growing "barbed" end of the filamentous (F) actin. Once in the filament, the ATP-actin hydrolyzes into ADP-actin quickly, resulting in an ATP cap at the barbed end composed of newly added subunits. The slow growing end of the F-actin is called the "pointed end", consisting of ADP-actin subunits. The concentration of G-actin resulting in net growth at a filament end is referred to as the "critical concentration" (Cc). If the G-actin concentration is below the Cc, disassembly will occur at that end. The pointed end of F-actin has a much higher Cc than the barbed end, and thus under steady-state conditions growth occurs at the barbed end and disassembly occurs at the pointed end. This is referred to as actin "treadmilling".

On its own, actin nucleation is an inefficient process. It is kinetically unfavorable due to the instability of the actin dimer (Goley and Welch, 2006). In order to achieve efficient actin polymerization, an actin nucleator must be employed.

Actin Nucleators and Nucleation Promoting Factors

Three types of actin nucleators have been identified: formins, Wasp-homology-2 domain (WH2) repeat proteins (spire and cordon-bleu), and the Arp2/3 complex (Campellone and Welch, 2010). Formins are the most diverse class of actin nucleators, with 15 mammalian formins having been identified (Schönichen and Geyer, 2010). The FH2 domain of formins is able to stabilize dimeric actin to promote the polymerization of long straight actin filaments. Formins remain bound to the barbed end of the filament as it grows, conferring protection from capping proteins which would prohibit further monomer addition (Kovar and Pollard, 2004; Zigmond et al. 2003). Actin filaments polymerized by formins tend to become bundled (Harris et al. 2006).

The WH2 repeat proteins also produce long, unbranched actin filaments by binding actin monomers and acting as a scaffold for nucleation. Spire contains four WH2 repeats, and cordon-bleu contains three (Renault et al., 2008). Spire has been reported to bind to the barbed end of the actin filament and cap it, and this occupation of the barbed end by spire can recruit formin to restart barbed end growth in a proposed "ping pong" mechanism (Montaville et al., 2014). Spire and cordon-bleu have been implicated in both nucleation and disassembly of actin filaments, as well as G-actin sequestration. Further studies must be completed before a definitive answer of their *in vivo* function is reached.

Branched actin filaments are produced by the Actin Related Protein 2/3 complex (Arp2/3). Arp2/3 is a seven subunit protein complex that binds to a pre-existing actin filament (the "mother" filament) and nucleates new actin "daughter" filaments at a ~78 degree angle from the mother filament (Rotty et al., 2013; Rouiller et al., 2008).

The Arp2/3 complex

The Arp2/3 complex was initially identified as an interacting protein for the actin binding protein profilin (Machesky et al., 1994). It was named "actin related protein" as two of its subunits, Arp2 and Arp3, resemble an actin dimer and form the seed for branch nucleation. The other 5 members of the Arp2/3 complex (ARPC1-5) provide structural framework and create the binding interface that contacts the mother filament (Fig 1.2).

The branched F-actin created by Arp2/3 has a critical role in the formation of the lamellipodium. In fact, in a 2012 paper from Wu et al, cells depleted of two subunits of Arp2/3 were unable to form lamellipodia (Wu et al., 2012). Instead, these cells were dominated by bundled filopodial structures. When Arp2/3 complex was re-introduced to these cells through microinjection of the protein, lamellipodia were restored (Fig 1.3).

The Arp2/3 complex is highly conserved in eukaryotes, and deletion of the Arp2/3 subunit in yeast, *Drosophila*, *C. elegans*, *Dictyostelium,* and mice is lethal (Schwob and Martin, 1992; Zallen et al., 2002; Sawa et al., 2003; Hudson and Cooley, 2002; Zaki et al., 2007; Yae et al., 2006). In addition to its role in lamellipodia formation and migration, Arp2/3 is involved in many other cellular processes (Fig 1.4). Phagocytosis, endocytosis, exocytosis, and endosomal fission all utilize Arp2/3 branched F-actin (Rotty et al., 2013). Arp2/3 is also found at adherens junctions (Han et al., 2014).

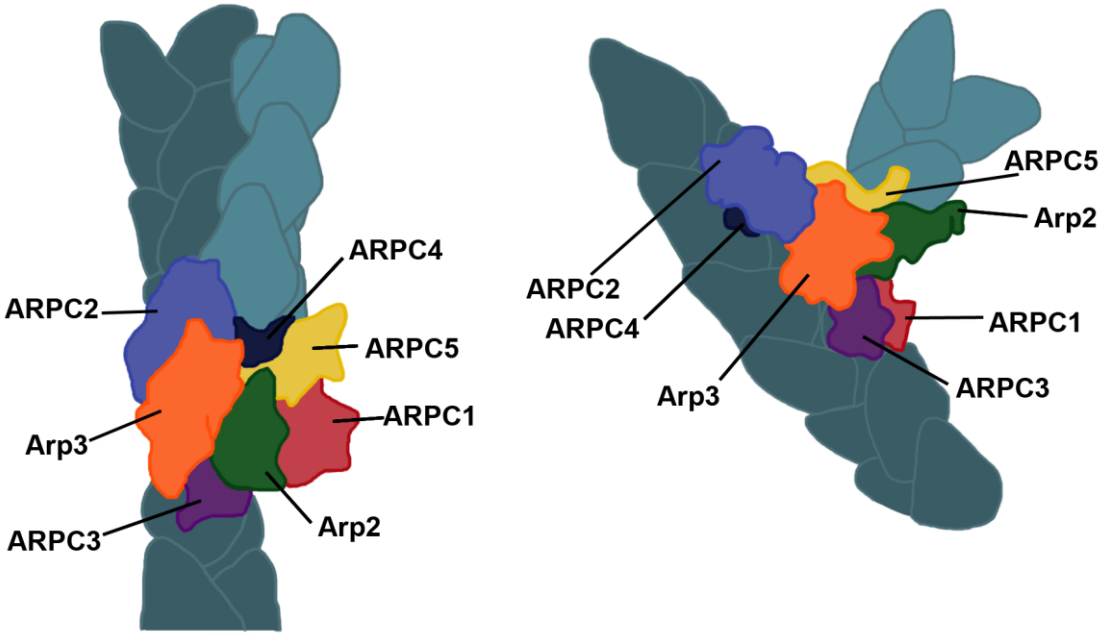

Figure 1.2 Arp2/3 is a 7 subunit complex that nucleates actin in Y shaped branches.

The Arp2/3 complex consists of 7 subunits. When activated by a NPF, Arp2 (green) and Arp3 (orange) shift into a position that allows nucleation of a new actin filament called a "branch" or "daughter filament" (in light blue) from a pre-existing "mother" filament (in dark blue). The other subunits provide structure and allow binding to the mother filament. Figure adapted from Rouiller et al., 2008)

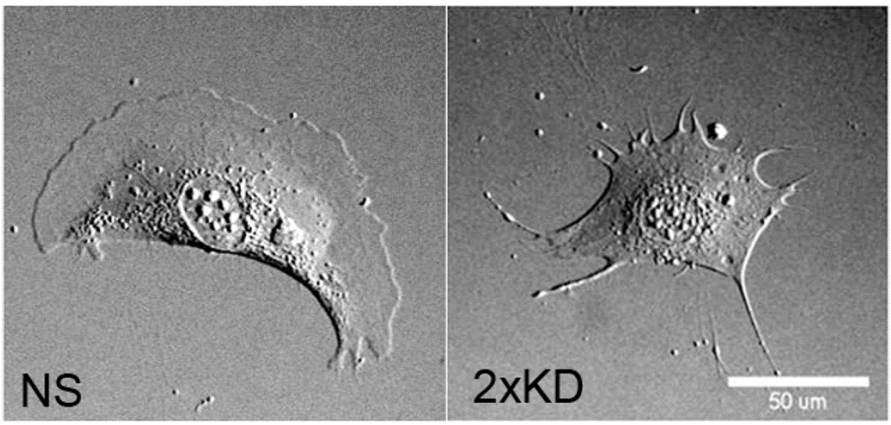

Figure 1.3 Arp2/3 complex is required for lamellipodia formation.

The cell on the left has been infected with a non-specific (NS) shRNA, while the cell on the right has been virally infected with two shRNAs against the ARPC2 and Arp2 subunits of Arp2/3 (2xKD). The broad, fan shaped lamellipodia containing branched actin, as seen on the left, is replaced by bundled actin structures resembling filopodia in the cell on the right. Modified from Wu and Asokan et al., 2012.

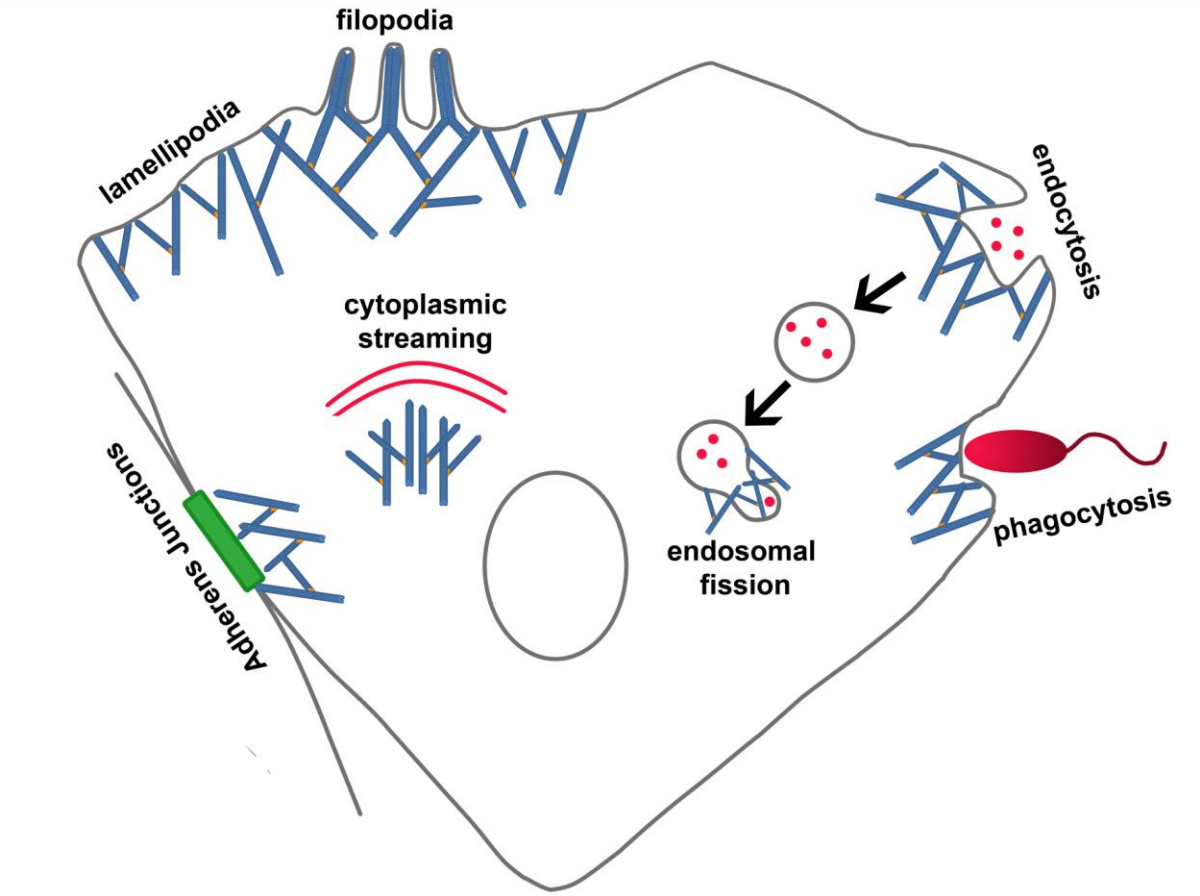

Figure 1.4 Arp2/3 is involved in many cellular processes.

Branched F-actin is utilized in many different cellular processes, included force generation for endocytosis, phagocytosis, and endosomal fission. It is critical for the formation of the lamellipodia and may seed bundled F-actin filopodial structures as well. Arp2/3 is found at adherens junctions and is utilized in the process of cytoplasmic streaming (Rotty et al., 2013).

Nucleation Promoting Factors

In vitro, Arp2/3 has little biochemical activity on its own. In order to nucleate new branches effectively, Arp2/3 must be activated by Nucleation Promoting Factors (NPFs). There are two classes of NPFs: type I and type II. Type II NPFs include cortactin and its hematopoetic homolog HS1, and will be discussed later in the section. Type I NPFs are quite diverse, but all contain a common WCA domain. The WCA domain consists of a WH2 (W) domain, a central connector (C), and an acidic region (A). The WCA domain alone is sufficient to activate Arp2/3 and lead to branch creation *in vitro*. Mammalian type I NPFs include WASP, N-WASP, SCAR/WAVE1-3, WASH, WHAMM and JMY. WASH and WHAMM do not act at the lamellipodia, but are involved in endosomal trafficking and the secretory pathway (Campellone et al., 2008; Duleh and Welch, 2010; Rottner et al., 2010). WASH in particular is an Arp2/3 activator for endosomes, whereas WHAMM is associated with the formation of tubulovesicular structures at the endoplasmic reticulum intermediate compartment (ERGIC) and cis-Golgi. JMY is unique in that it is the first NPF identified with independent actin nucleation activity (Zuchero et al., 2009). Though JMY has been seen to localize to the lamellipodia, its role in lamellipodial actin polymerization is not well-studied. Instead, work thus far has focused on its role as a regulator of p53 signaling (Coutts et al., 2009).

The main players in the control of activating the Arp2/3 complex at the leading edge are WASP, N-WASP, and the WAVEs (Fig 1.5). WASP expression is confined to cells of hematopoietic lineage, while N-WASP is ubiquitously expressed (Snapper and Rosen, 2009). Mutation of WASP in humans results in the immune disease Wiscott-Aldrich Syndrome,

while deletion of N-WASP in mice is associated with cardiac and neuronal abnormalities and embryonic lethality (Snapper and Rosen, 1999; Dahl et. al., 2003).

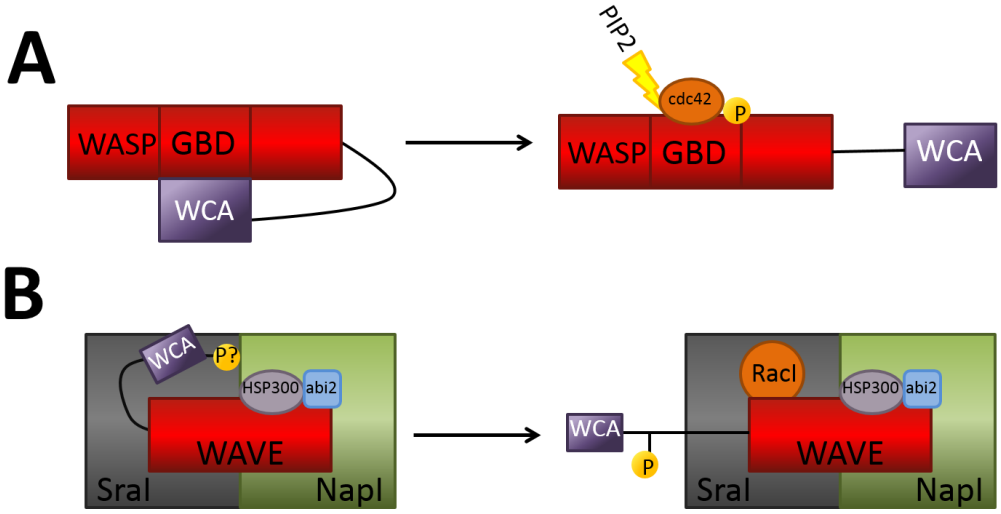

Figure 1.5 Activation of NPFs by various stimuli.

SCAR/WAVE (A) and WASP/N-WASP (B) are the two main NPFs which activate Arp2/3 at the membrane to control migration. While both share a WCA domain, WASP/N-WASP has an autoinhibitory GBD domain which WAVE does not share. Instead, WAVE is maintained inactive in a complex until Rac binding. Relief of WASP's autoinhibition occurs through PtdIns(4,5)P2 and cdc42 binding.

WASP and N-WASP (hereafter collectively referred to as WASP) are autoinhibited by the binding of the WCA domain to the GTPase-binding domain (GBD) (Kim et al., 2000). This autoinhibition can be relieved by cooperative binding of the activated GTPase CDC42 and phosphatidylinositol (4,5)-bisphosphate (PtdIns(4,5)P2) to the GBD domain and basic region of WASP (Fig 1.5 A). Once active, the WCA region of WASP can bind to Arp2/3 at two sites: one on Arp3, and one which spans Arp2 and ARPC1. Recent work suggests two WCA domains may be able to bind Arp2/3 at the same time using these two distinct sites (Helgeson and Nolen, 2013; Ti et al., 2011; Padrick et al., 2011). Upon binding WASP causes a conformational change in Arp2/3 and contributes an actin monomer. The conformational

change allows the Arp2 and Arp3 subunits to form an intermediate resembling dimeric actin, and the addition of an actin monomer forms the complete nucleus for daughter filament growth. Recent work indicates that activation of Arp2/3 complex occurs prior to mother filament binding, and that the WCA domain is released prior to daughter filament polymerization (Smith et al., 2013). Nucleation also triggers ATP hydrolysis on Arp2 (Dayel and Mullins, 2004).

Unlike WASP, WAVEs do not have an autoinhibitory domain. Instead, a protein complex consisting of SRA1, NAP1, HSP300, and ABI2 confines WAVE to an inactive state (Rotty et al., 2013) (Fig 1.5 B). This inhibition can be relieved either by phosphorylation of WAVE by various kinases or binding of the GTPase Rac1. Once the WCA domain is free to bind Arp2/3, the mechanism of activation of Arp2/3 by WAVE is the same as with WASP.

Type II NPFs lack a complete WCA domain, but possess an N-terminal acidic region which can bind to Arp2/3, as well as a series of F-actin (but not G-actin) binding repeats. Type II NPFs only weakly activate Arp2/3 on their own, though cortactin displacement of N-WASP on Arp2/3 accelerates the rate of nucleation, as release of WCA from Arp2/3 is the rate-limiting step of branch nucleation (Helgeson and Nolen, 2013). Once WCA is released from Arp2/3, cortactin remains associated with the branch and stabilizes it.

Hydrolysis of ATP by the Arp2 or Arp3 subunit occurs at the same time as a branch is nucleated. Arp2 an Arp3 both have ATP binding pockets, though these have 1,000x less affinity for ATP than G-actin (Dayel et al., 2001). ATP hydrolysis by Arp2 or Arp3 does not appear to be important for nucleation, but work done with non-hydrolyzing Arp2 and Arp3 mutants show its importance in disassembly (Ingerman et al., 2013). In cells, the front-to-

back width of the branched actin network increases with a non-hydrolyzing mutants of Arp2/3.

Actin disassembly and debranching

In vitro F-actin branches remain stable for between 8 and 27 minutes (Mahaffy and Pollard, 2006; Martin et al., 2006). This lifetime is not compatible with observed cell behavior, where cells must quickly reorganize their F-actin cytoskeleton to respond to external stimuli. These observations led to speculations that there must exist *debranching* proteins that would destabilize and turn over branched filaments.

Actin disassembly can occur spontaneously in steady state conditions, as the ADP actin at the pointed end is dissociated from the filament. It can also occur with the help of Actin Depolymerizing Factor (ADF)/cofilin proteins. While ADF and cofilin do have slight differences in activity, cofilin is the more ubiquitous protein and its knockout is lethal in mice, therefore this discussion will focus on cofilin (Gurniak et al., 2005; Bernstein and Bamburg, 2010). Cofilin's role in the cell is complex and its activity is influenced by many other cytoskeletal proteins. Cofilin activity is inhibited by phosphorylation on ser3 by LIM and TES kinases, and this inhibition can be relieved by either of two phosphatases (SSH1L and chronophin) (Nagata-Ohashi et al., 2004; Gohla et al., 2005; Van Troys et al., 2008).

Cofilin binding to F-actin at low occupancy leads to a conformational change in the filament that results in filament severing (Andrianantoandro and Pollard, 2006). This severing can contribute to the generation of new actin monomers and new barbed ends for filament growth. Therefore, disassembly is integral for continued actin polymerization. Cofilin is also theorized to lead to debranching in two ways (Chan et al., 2009). The first occurs through cofilin increasing the speed of conversion from ADP-P_i-actin to ADP-actin.

Arp2/3 has less affinity for ADP-actin, and so dissociation of Arp2/3 from the mother filament may occur more quickly. The second mechanism is more direct: the mother filament becomes saturated with cofilin and changes conformation enough to cause dissociation of the Arp2/3 complex from the mother filament. It has also been observed that non-hydrolyzing mutants of Arp2/3 take longer to undergo cofilin-mediated disassembly (Ingerman et al., 2013). While these mechanisms have been seen *in vitro*, direct evidence supporting either mechanism *in vivo* is not available. Furthermore, the physiological probability of rapidly achieving high occupation of a filament by cofilin without transit through a low occupancy state (thus encouraging severing) has not been established. Therefore, more potent debranching factors than cofilin may be more relevant *in vivo*.

Coronin1B has been reported to cause actin filament debranching in fibroblasts through replacement of Arp2/3 at the branch junction. This increases the angle of the daughter branch from the mother filament and results in branch dissociation (Cai et al., 2008). Coronin1B also antagonizes cortactin and helps to direct SSH1L to the leading edge (Cai et al., 2007). SSH1L is able to remove the inhibitory ser3 phosphorylation from cofilin, making it more active at the leading edge, and thus able to contribute to debranching and disassembly of branched actin.

In addition to coronin1B, work in the last ~10 years on an ADF/cofilin family protein called Glia Maturation Factor (GMF) has identified it as an Arp2/3 interacting protein and a debranching factor (Gandhi et al., 2010).

Glia Maturation Factor

GMF was identified in the late 1980's from bovine brain extract (Lim et al., 1989). Initial experiments identified it as a secreted brain-specific growth factor. Further work by

the same group implicated the protein in inflammation and neurological diseases like Alzheimer's. However, sequence analysis later lead to the discovery that GMF had high sequence homology with cofilin (Walker, 2003). Studies performed on yeast GMF1 identified it as an Arp2/3 binding protein, and showed its association with actin patches (Nakano et al., 2010; Gandhi et al., 2010). Nakano et al. first showed by pull-down assay that GMF1 associated with Arp2/3, but not actin. Secondly, they performed both *in vitro* TIRF assays and pyrene-labeled actin assays, where they observed that upon addition of GMF1 to the reaction, actin assembly was antagonized. Gandhi et al. also performed pyrene-labeled actin assays, and found increasing concentrations of GMF1 promoted disassembly of existing F-actin. These changes only occurred in the presence of Arp2/3 complex and VCA, unbranched actin was not affected by GMF1.

Using live TIRF imaging, Gandhi et al. found when GMF1 was added *in vitro* to pre-polymerized branched actin filaments, dissociation of the daughter filament could be observed (Gandhi et al., 2010). These groups also found evidence that GMF1 competed with WASP/WAVE for Arp2/3 binding or could otherwise inhibit nucleation of daughter filaments (Nakano et al., 2010; Gandhi et al., 2010). These results led to the generation of two hypotheses on how GMF antagonizes Arp2/3: direct destabilization of the branch by its binding to Arp2/3, and/or preventing Arp2/3 from becoming activated by NPFs through binding site competition (Ydenberg et al., 2013; Luan and Nolen, 2013). These hypotheses are not mutually exclusive, and could each contribute to GMF's net effect on branched F-actin.

Two isoforms of mammalian GMF have been discovered: GMFβ and GMFγ. GMFβ has primarily been the subject of research implicating it as a brain-specific factor, although

RNA-seq data indicates that it appears to be expressed ubiquitously in various cell types. GMFγ has more restricted expression in cells of hematapoetic lineage, and has been more heavily studied as a cytoskeletal protein.

The first report that a GMF isoform (GMFγ) was important outside of the brain began as a screen to find genes preferentially expressed in endothelial cells (Ikeda et al., 2006). GMFγ appeared highly expressed in microvascular endothelial cells and inflammatory cells, but not neuronal cells, and had high sequence homology to cofilin. Expression of GMFγ in bovine aortic endothelial cells (BAECs) showed its localization to the lamellipodia, increased cell motility, and enhanced lamellipodial activity (Ikeda et al., 2006). GMFγ was also identified in the leading edge of neutrophils during chemotaxis (Aerbajinai et al., 2011). Interestingly, depletion of GMFγ interrupted cells' ability to polarize to a chemoattractant, instead resulting in multiple misdirected protrusions around the cell. Likewise, another study in T-lymphocytes showed disruption in migration speed and chemotactic ability of cells depleted of GMFγ, which was attributed to an increase in substrate adherence and α5β1 integrin expression (Lippert and Wilkins, 2012). GMFγ has also been implicated in endocytic trafficking in macrophages (Aerbajinai et al., 2013).

At this time, there has been limited research on GMF in animals. A 2013 study in zebrafish found GMFγ was important for angiogenic sprouting (Zuo et al., 2013). Zebrafish injected with a GMFγ morpholino had severely reduced angiogenic sprouting, but those injected with a GMFβ morpholino retained a normal sprouting phenotype. In *Drosophila*, dGMF was studied in border cell migration dynamics (Poukkula et al., 2014). It was found that in the early stages of border cell migration, depletion of dGMF results in slower migration speeds, increased protrusion lifetime, and reduced protrusion size. In *Drosophila*

S2 cell cultures, depletion of dGMF resulted in increased accumulation of actin around the edge of the cell. The effect of dGMF depletion was exaggerated by depletion of AIP1, an enhancer of cofilin activity. A GMFβ knockout mouse has been published, however the cytoskeletal implications of this GMFβ knockout have not been addressed (Lim et al., 2004). This mouse exhibits a reduced number of neurons in the inferior olive, leading to defects in motor skills and motor learning in tasks like beam walking and eyeblink response conditioning (Lim et al., 2004). GMFβ depletion is also reported to be anti-inflammatory, reducing cytokine production in the brain after pro-inflammatory insult (encephalitis or 1-methyl-4-phenyl-1,2,3,6-tetrahydropyridine treatment) (Zaheer et al., 2007; Khan et al., 2015).

Structural Elements of GMF and Proposed Mechanisms

The crystal structure of mouse GMFγ bound to Arp2/3 complex was solved in 2013, providing insight into the mechanism of GMF's action on Arp2/3 (Fig. 6) (Luan and Nolen, 2013). GMFγ's major contact site is on the barbed end of Arp2, one of the Arp2/3 subunits which makes the nucleus for new filament growth. Interestingly, the association with the barbed end of the Arp2 subunit is reminiscent of cofilin's mode of binding to the barbed end of actin. The N-terminus of GMFγ is shifted in the Arp2/3 bound state when compared to the unbound state and interacts with subdomain 1 of Arp2. The α3 helix of GMFγ is buried inside the barbed end groove of Arp2, and is also shifted in the bound state vs. the unbound state. GMFγ also contacts ARPC1, however the residues involved in this interaction are not well conserved across species, suggesting that this interaction is not as important as that with Arp2. Chemical crosslinking analysis also supports the interaction of GMF with Arp2 and

ARPC1, but additionally suggests interaction with Arp3, which is not supported by crystal structure data (Ydenberg et al., 2013).

An important observation from the structure of GMFγ bound to Arp2/3 is that GMFγ overlaps with one of the two NPF CA binding sites of the Arp2/3 complex. The CA of NPF's WCA domain has been shown by crosslinking to contact ARPC1 and Arp2, just as GMFγ does. This agrees with previous data demonstrating GMF's ability to compete with NPFs, although pyrene actin polymerization experiments have been unable to demonstrate significant nucleation inhibition by GMFγ (Boczkowska et al., 2013).

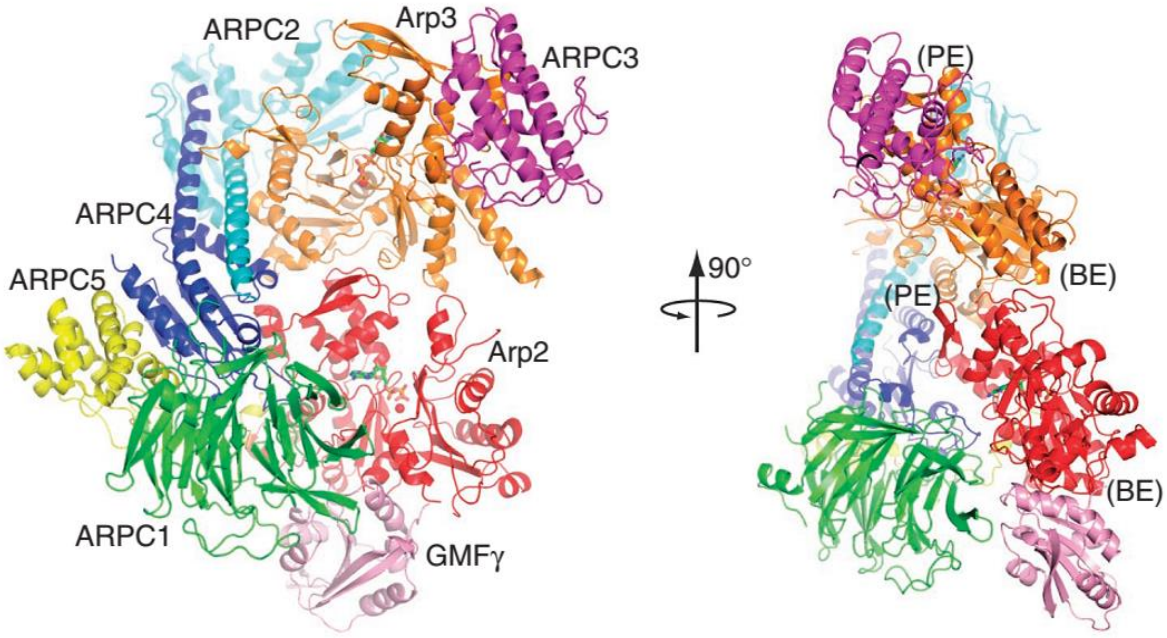

Figure 1.6 Structure of GMFγ bound to the Arp2/3 complex.

Ribbon diagram of *Bos taurus* Arp2/3 complex (PDB 1TYQ) with bound *Mus musculus* GMFγ, ATP and calcium. (from Luan and Nolen, 2013, PDB 4JD2). GMF (pink) binds the barbed end of Arp2 (red) and also contacts ARPC1 (green). The barbed and pointed ends of Arp2 and Arp3 are labeled (BE) or (PE), respectively.

The binding site for GMFγ on Arp2 is accessible even when Arp2/3 complex is in an existing branch (Luan and Nolen, 2013; Ydenberg et al., 2013). When binding Arp2/3 in a branch, GMFγ is able to contact Arp2 as well as the adjacent actin monomer in a similar manner to cofilin binding of F-actin. Therefore, it is proposed that GMFγ uses a modified cofilin mechanism to sever Arp2/3 branched actin filaments at the daughter filament junction. In support of this mechanism, mutation of a set of three highly conserved amino acids in the region of yeast GMF1 that is proposed to contact the first actin subunit of the daughter filament results in severe defects in debranching (Ydenberg et al., 2013). This mutant did not affect NPF competition.

While the mechanisms of GMF's function as an Arp2/3 antagonist have been elucidated, there has not been any definitive work on whether direct debranching or NPF competition is the dominant mode of action *in vivo.* However, mutational analysis in yeast did show that GMF1 mutants deficient in NPF competition activity had normal growth rates, unlike mutations targeting debranching activity (Ydenberg et al., 2013).

Regulation of GMF

Due to GMF's homology to cofilin, it was assumed that N-terminal serines present on GMF would be regulatory. Early work in mouse GMFγ used P^{32} labeling to detect phosphorylation of GMFγ, which was ablated when the N-terminal serines (S2, S4) were mutated to alanine (Ikeda et al., 2006). Building from this observation, Nakano et al found that the phosphomimetic mutant of GMFγ (S2E) had a milder Arp2/3-antagonizing activity than the wild type (WT) GMFγ (Nakano et al., 2010). A phosphomimetic mutant of yeast GMF1 (S2E) was strongly deficient in NPF competition, but had a growth rate and

debranching ability comparable to WT (Ydenberg et al., 2013). The non-phosphorylatable mutant (S2A) had a WT growth rate and no reported defects.

GMFγ has been reported to bind with higher affinity to ADP-Arp2/3 than ATP-Arp2/3, suggesting that it prefers to bind Arp2/3 after branch nucleation (Boczkowska et al., 2013). A GMFγ-S2E mutant had reduced affinity for binding to ADP-Arp2/3, and in fact displayed a similar level of affinity as that observed for WT GMFγ bound to ATP-Arp2/3. In conflict with these findings, no structural evidence for GMF regulation by Ser2 phosphorylation could be detected in the solved crystal structure of Arp2/3 bound by GMFγ (Luan and Nolen, 2013).

Finally, a recent paper suggests Tyr-104 phosphorylation mediated by c-Abl tyrosine kinase inhibits GMFγ's association with Arp2/3 (Wang et al., 2014). This is the only report indicating the importance of this residue, although it is highly conserved. Mutational analysis in yeast (Y110F) resulted in a WT growth rate and no reported defects (Ydenberg et al., 2013).

There is still significant work to be done on the regulation and targeting of GMF, especially since there is no clear consensus in the literature regarding the importance of the phosphorylation sites that have been studied. No kinases or phosphatases have been confirmed to target GMFγ (outside of c-Abl). Control of GMF by ubiquitination or sequestration of GMF, or by phosphorylation state of Arp2/3, has been completely unexplored.

GMF's interactions with other cytoskeletal proteins is also a largely unexplored field. Coronins have been implicated as GMF interacting proteins through immunoprecipitation, and functional synergy with AIP1 has been observed in *Drosophila*. How GMF interacts with

cortactin, and the physiological differences between cofilin, coronin, and GMF in debranching are all exciting questions waiting to be resolved.

REFERENCES

1. Aerbajinai, W., K. Lee, K. Chin, and G.P. Rodgers. 2013. Glia maturation factor-γ negatively modulates TLR4 signaling by facilitating TLR4 endocytic trafficking in macrophages. *J. Immunol.* 190:6093–103. doi:10.4049/jimmunol.1203048.

2. Aerbajinai, W., L.H. Liu, K. Chin, J.Q. Zhu, C.A. Parent, and G.P. Rodgers. 2011. Glia maturation factor-gamma mediates neutrophil chemotaxis. *J. Leukoc. Biol.* 90:529–538. doi:Doi 10.1189/Jlb.0710424.
3. Aman, A., and T. Piotrowski. 2010. Cell migration during morphogenesis. *Dev. Biol.* 341:20–33. doi:10.1016/j.ydbio.2009.11.014.

4. Andrianantoandro, E., and T.D. Pollard. 2006. Mechanism of Actin Filament Turnover by Severing and Nucleation at Different Concentrations of ADF/Cofilin. *Mol. Cell*. 24:13–23. doi:10.1016/j.molcel.2006.08.006.

5. Asokan, S.B., H.E. Johnson, A. Rahman, S.J. King, J.D. Rotty, I.P. Lebedeva, J.M. Haugh, and J.E. Bear. 2014. Mesenchymal Chemotaxis Requires Selective Inactivation of Myosin II at the Leading Edge via a Noncanonical PLCγ/PKCα Pathway. *Dev. Cell*. 31:747–760. doi:http://dx.doi.org/10.1016/j.devcel.2014.10.024.

6. Bear, J.E., and J.M. Haugh. 2014. Directed migration of mesenchymal cells: Where signaling and the cytoskeleton meet. *Curr. Opin. Cell Biol.* 30:74–82. doi:10.1016/j.ceb.2014.06.005.

7. Bernstein, B.W., and J.R. Bamburg. 2010. ADF/Cofilin: A functional node in cell biology. *Trends Cell Biol.* 20:187–195. doi:10.1016/j.tcb.2010.01.001.

8. Boczkowska, M., G. Rebowski, and R. Dominguez. 2013. Glia maturation factor (GMF) interacts with Arp2/3 complex in a nucleotide state-dependent manner. *J Biol Chem*. 288:25683–25688. doi:C113.493338 [pii] 10.1074/jbc.C113.493338.

9. Cai, L., A.M. Makhov, D.A. Schafer, and J.E. Bear. 2008. Coronin 1B antagonizes Cortactin and remodels Arp2/3-containing actin branches in lamellipodia. *Cell*. 134:828–842. doi:10.1016/j.cell.2008.06.054.

10. Cai, L., T.W. Marshall, A.C. Uetrecht, D.A. Schafer, and J.E. Bear. 2007. Coronin 1B coordinates Arp2/3 complex and Cofilin activities at the leading edge. *Cell*. 128:915–929. doi:10.1016/j.cell.2007.01.031.

11. Campellone, K.G., N.J. Webb, E.A. Znameroski, and M.D. Welch. 2008. WHAMM Is an Arp2/3 Complex Activator That Binds Microtubules and Functions in ER to Golgi Transport. *Cell*. 134:148–161. doi:10.1016/j.cell.2008.05.032.

12. Campellone, K.G., and M.D. Welch. 2010. A nucleator arms race: cellular control of actin assembly. *Nat. Rev. Mol. Cell Biol.* 11:237–251. doi:10.1038/nrm2867.

13. Chan, C., C.C. Beltzner, and T.D. Pollard. 2009. Cofilin Dissociates Arp2/3 Complex and Branches from Actin Filaments. *Curr. Biol.* 19:537–545. doi:10.1016/j.cub.2009.02.060.

14. Coutts AS, Weston L, La Thangue NB. 2009. A transcription co-factor integrates cell adhesion and motility with the p53 response. *PNAS*. 106(47):19872-7. doi: 10.1073/pnas.0906785106.

15. Dahl J. P., Wang-Dunlop J., Gonzales C., Goad M. E., Mark R. J., Kwak S. P. 2003. Characterization of the WAVE1 knock-out mouse: implications for CNS development. *J. Neurosci*. 23:3343–3352.

16. Dayel, M.J., E.A. Holleran, and R.D. Mullins. 2001. Arp2/3 complex requires hydrolyzable ATP for nucleation of new actin filaments. *Proc. Natl. Acad. Sci. U. S. A.* 98:14871–14876. doi:10.1073/pnas.261419298.

17. Dayel, M.J., and R.D. Mullins. 2004. Activation of Arp2/3 complex: Addition of the first subunit of the new filament by a WASP protein triggers rapid ATP hydrolysis on Arp2. *PLoS Biol.* 2. doi:10.1371/journal.pbio.0020091.

18. Duleh, S.N., and M.D. Welch. 2010. WASH and the Arp2/3 complex regulate endosome shape and trafficking. *Cytoskeleton*. 67:193–206. doi:10.1002/cm.20437.

19. Gandhi, M., B.A. Smith, M. Bovellan, V. Paavilainen, K. Daugherty-Clarke, J. Gelles, P. Lappalainen, and B.L. Goode. 2010. GMF is a cofilin homologue that binds Arp2/3 complex to stimulate filament debranching and inhibit actin nucleation. *Curr. Biol.* 20:861–867. doi:10.1016/j.cub.2010.03.026.

20. Gohla, A., J. Birkenfeld, and G.M. Bokoch. 2005. Chronophin, a novel HAD-type serine protein phosphatase, regulates cofilin-dependent actin dynamics. *Nat. Cell Biol.* 7:21–29. doi:10.1038/ncb1201.

21. Goley, E.D., and M.D. Welch. 2006. The ARP2/3 complex: an actin nucleator comes of age. *Nat. Rev. Mol. Cell Biol.* 7:713–726. doi:10.1038/nrm2026.

22. Gurniak, C.B., E. Perlas, and W. Witke. 2005. The actin depolymerizing factor n-cofilin is essential for neural tube morphogenesis and neural crest cell migration. *Dev. Biol.* 278:231–241. doi:10.1016/j.ydbio.2004.11.010.

23. Han, S.P., Y. Gambin, G.A. Gomez, S. Verma, N. Giles, M. Michael, S.K. Wu, Z. Guo, W. Johnston, E. Sierecki, R.G. Parton, K. Alexandrov, and A.S. Yap. 2014. Cortactin scaffolds Arp2/3 and WAVE2 at the epithelial zonula adherens. *J. Biol.*

Chem. 289:7764–7775. doi:10.1074/jbc.M113.544478.

24. Harris, E.S., Rouiller I., Hanein D., Higgs H.N. 2006. Mechanistic differences in actin bundling activity of two mammalian formins, FRL1 and mDia2. *J. Biol. Chem.* 281(20):14383-92

25. Helgeson, L.A., and B.J. Nolen. 2013. Mechanism of synergistic activation of Arp2/3 complex by cortactin and N-WASP. *Elife*. 2013. doi:10.7554/eLife.00884.

26. Hudson, A.M., and L. Cooley. 2002. A subset of dynamic actin rearrangements in Drosophila requires the Arp2/3 complex. *J. Cell Biol.* 156:677–687. doi:10.1083/jcb.200109065.

27. Ikeda, K., R.K. Kundu, S. Ikeda, M. Kobara, H. Matsubara, and T. Quertermous. 2006. Glia maturation factor-gamma is preferentially expressed in microvascular endothelial and inflammatory cells and modulates actin cytoskeleton reorganization. *Circ Res*. 99:424–433. doi:01.RES.0000237662.23539.0b [pii] 10.1161/01.RES.0000237662.23539.0b.

28. Ingerman, E., J.Y. Hsiao, and R.D. Mullins. 2013. Arp2/3 complex ATP hydrolysis promotes lamellipodial actin network disassembly but is dispensable for assembly. *J. Cell Biol.* 200:619–633. doi:10.1083/jcb.201211069.

29. Kim, A.S., L.T. Kakalis, N. Abdul-Manan, G.A. Liu, and M.K. Rosen. 2000. Autoinhibition and activation mechanisms of the Wiskott-Aldrich syndrome protein. *Nature*. 404:151–158. doi:10.1038/35004513.

30. Kovar, D.R. and T. Pollard. 2004. Insertional assembly of actin filament barbed ends in association with formins produces piconewton forces. *PNAS.* 101(41): 14725–14730. doi:10.1073/pnas.0405902101

31. Lambrechts, a, M. Van Troys, and C. Ampe. 2004. The actin cytoskeleton in normal and pathological cell motility. *Int. J. Biochem. Cell Biol.* 36:1890–1909. doi:10.1016/j.biocel.2004.01.024.

32. Lämmermann, T., and M. Sixt. 2009. Mechanical modes of "amoeboid" cell migration. *Curr. Opin. Cell Biol.* 21:636–644. doi:10.1016/j.ceb.2009.05.003.

33. Lim, R., J.F. Miller, and A. Zaheer. 1989. Purification and characterization of glia maturation factor beta: a growth regulator for neurons and glia. *Proc. Natl. Acad. Sci. U. S. A.* 86:3901–3905.

34. Lim, R., A. Zaheer, H. Khosravi, J.H. Freeman, H.E. Halverson, J.A. Wemmie, and B. Yang. 2004. Impaired motor performance and learning in glia maturation factor-knockout mice. *Brain Res.* 1024:225–232. doi:10.1016/j.brainres.2004.08.003.

35. Lippert, D.N., and J.A. Wilkins. 2012. Glia maturation factor gamma regulates the migration and adherence of human T lymphocytes. *BMC Immunol*. 13:21. doi:1471-2172-13-21 [pii] 10.1186/1471-2172-13-21.

36. Luan, Q., and B.J. Nolen. 2013. Structural basis for regulation of Arp2/3 complex by GMF. *Nat. Struct. Mol. Biol.* 20:1062–1068. doi:10.1038/nsmb.2628.

37. Machesky, L. M., Atkinson, S. J., Ampe, C.,Vandekerckhove, J. & Pollard, T. D. 1994. Purification of a cortical complex containing two unconventional actins from Acanthamoeba by affinity chromatography on profilin-agarose. *J. Cell Biol.* 127:107–115.

38. Mahaffy, R.E., and T.D. Pollard. 2006. Kinetics of the formation and dissociation of actin filament branches mediated by Arp2/3 complex. *Biophys. J.* 91:3519–3528. doi:10.1529/biophysj.106.080937.

39. Martin, A.C., M.D. Welch, and D.G. Drubin. 2006. Arp2/3 ATP hydrolysis-catalysed branch dissociation is critical for endocytic force generation. *Nat. Cell Biol.* 8:826–833. doi:10.1038/ncb1443.

40. Montaville, P., A. Jégou, J. Pernier, C. Compper, B. Guichard, B. Mogessie, M. Schuh, G. Romet-Lemonne, and M.F. Carlier. 2014. Spire and Formin 2 Synergize and Antagonize in Regulating Actin Assembly in Meiosis by a Ping-Pong Mechanism. *PLoS Biol.* 12. doi:10.1371/journal.pbio.1001795.

41. Nagata-Ohashi, K., Y. Ohta, K. Goto, S. Chiba, R. Mori, M. Nishita, K. Ohashi, K. Kousaka, A. Iwamatsu, R. Niwa, T. Uemura, and K. Mizuno. 2004. A pathway of neuregulin-induced activation of cofilin-phosphatase Slingshot and cofilin in lamellipodia. *J. Cell Biol.* 165:465–471. doi:10.1083/jcb.200401136.

42. Nakano, K., H. Kuwayama, M. Kawasaki, O. Numata, and M. Takaine. 2010. GMF is an evolutionarily developed Adf/cofilin-super family protein involved in the Arp2/3 complex-mediated organization of the actin cytoskeleton. *Cytoskelet.* 67:373–382. doi:10.1002/cm.20451.

43. Padrick, S.B., L.K. Doolittle, C.A. Brautigam, D.S. King, and M.K. Rosen. 2011. Arp2/3 complex is bound and activated by two WASP proteins. *Proc. Natl. Acad. Sci. U. S. A.* 108:E472–E479. doi:10.1073/pnas.1100236108.

44. Poukkula, M., M. Hakala, N. Pentinmikko, M.O. Sweeney, S. Jansen, J. Mattila, V. Hietakangas, B.L. Goode, and P. Lappalainen. 2014. GMF Promotes Leading-Edge Dynamics and Collective Cell Migration In Vivo. *Curr Biol*. 24:2533–2540. doi:S0960-9822(14)01130-0 [pii] 10.1016/j.cub.2014.08.066.

45. Renault, L., B. Bugyi, and M.F. Carlier. 2008. Spire and Cordon-bleu: multifunctional regulators of actin dynamics. *Trends Cell Biol.* 18:494–504.

doi:10.1016/j.tcb.2008.07.008.

46. Rottner, K., J. Hänisch, and K.G. Campellone. 2010. WASH, WHAMM and JMY: Regulation of Arp2/3 complex and beyond. *Trends Cell Biol.* 20:650–661. doi:10.1016/j.tcb.2010.08.014.

47. Rotty, J.D., C. Wu, and J.E. Bear. 2013. New insights into the regulation and cellular functions of the ARP2/3 complex. *Nat Rev Mol Cell Biol*. 14:7–12.

48. Rouiller, I., X.-P. Xu, K.J. Amann, C. Egile, S. Nickell, D. Nicastro, R. Li, T.D. Pollard, N. Volkmann, and D. Hanein. 2008. The structural basis of actin filament branching by the Arp2/3 complex. *J. Cell Biol.* . 180 :887–895. doi:10.1083/jcb.200709092.

49. Sawa, M., S. Suetsugu, A. Sugimoto, H. Miki, M. Yamamoto, and T. Takenawa. 2003. Essential role of the C. elegans Arp2/3 complex in cell migration during ventral enclosure. *J Cell Sci*. 116:1505–1518.

50. Schönichen, A., and M. Geyer. 2010. Fifteen formins for an actin filament: A molecular view on the regulation of human formins. *Biochim. Biophys. Acta - Mol. Cell Res.* 1803:152–163. doi:10.1016/j.bbamcr.2010.01.014.

51. Schwob, E., and R.P. Martin. 1992. New yeast actin-like gene required late in the cell cycle. *Nature*. 355:179–182. doi:10.1038/355179a0.

52. Smith, B.A., S.B. Padrick, L.K. Doolittle, K. Daugherty-Clarke, I.R. Corrêa, M.Q. Xu, B.L. Goode, M.K. Rosen, and J. Gelles. 2013. Three-color single molecule imaging shows WASP detachment from Arp2/3 complex triggers actin filament branch formation. *Elife*. 2013. doi:10.7554/eLife.01008.

53. Snapper, S.B., F.S. Rosen. 1999. The Wiskott-Aldrich syndrome protein (WASP): roles in signaling and cytoskeletal organization. *Annu. Rev. Immunol.* 17:905-29.

54. Ti, S.-C., C.T. Jurgenson, B.J. Nolen, and T.D. Pollard. 2011. Structural and biochemical characterization of two binding sites for nucleation-promoting factor WASp-VCA on Arp2/3 complex. *Proc. Natl. Acad. Sci. U. S. A.* 108:E463–E471. doi:10.1073/pnas.1100125108.

55. Van Troys, M., L. Huyck, S. Leyman, S. Dhaese, J. Vandekerkhove, and C. Ampe. 2008. Ins and outs of ADF/cofilin activity and regulation. *Eur. J. Cell Biol.* 87:649–667. doi:10.1016/j.ejcb.2008.04.001.

56. Walker, M.G. 2003. Gene expression versus sequence for predicting function: Glia Maturation Factor gamma is not a glia maturation factor. *Genomics, proteomics Bioinforma. / Beijing Genomics Inst.* 1:52–57.

57. Wang, T., R.A. Cleary, R. Wang, and D.D. Tang. 2014. GMF-γ Phosphorylation at Tyr-104 Regulates Actin Dynamics and Contraction in Human Airway Smooth Muscle. *Am. J. Respir. Cell Mol. Biol.* doi:10.1165/rcmb.2014-0125OC.

58. Wickramarachchi, D.C., A.N. Theofilopoulos, and D.H. Kono. 2010. Immune pathology associated with altered actin cytoskeleton regulation. *Autoimmunity*. 43:64–75. doi:10.3109/08916930903374634.

59. Wu, C., S.B. Asokan, M.E. Berginski, E.M. Haynes, N.E. Sharpless, J.D. Griffith, S.M. Gomez, and J.E. Bear. 2012. Arp2/3 is critical for lamellipodia and response to extracellular matrix cues but is dispensable for chemotaxis. *Cell*. 148:973–987.

60. Yae, K., V.W. Keng, M. Koike, K. Yusa, M. Kouno, Y. Uno, G. Kondoh, T. Gotow, Y. Uchiyama, K. Horie, and J. Takeda. 2006. Sleeping beauty transposon-based phenotypic analysis of mice: lack of Arpc3 results in defective trophoblast outgrowth. *Mol. Cell. Biol.* 26:6185–6196. doi:10.1128/MCB.00018-06.

61. Ydenberg, C.A., S.B. Padrick, M.O. Sweeney, M. Gandhi, O. Sokolova, and B.L. Goode. 2013. GMF severs actin-Arp2/3 complex branch junctions by a cofilin-like mechanism. *Curr. Biol.* 23:1037–1045. doi:10.1016/j.cub.2013.04.058.

62. Khan, M. M., S. Zaheer, R. Thangavel, M. Patel, D. Kempuraj, A. Zaheer. 2015. Absence of glia maturation factor protects dopaminergic neurons and improves motor behavior in mouse model of parkinsonism. *Neurochem. Res*. 40(5):980-90. doi: 10.1007/s11064-015-1553-x.

63. Zaheer, A., S. K. Sahu, Y. Wu, A. Zaheer, J. Haas, K. Lee, B. Yang. 2007. Diminished cytokine and chemokine expression in the central nervous system of GMF-deficient mice with experimental autoimmune encephalomyelitis. *Brain Research.* 1144 (2007) 239–247. doi:10.1016/j.brainres.2007.01.075.

64. Zaki, M., J. King, K. Fütterer, and R.H. Insall. 2007. Replacement of the essential Dictyostelium Arp2 gene by its Entamoeba homologue using parasexual genetics. *BMC Genet.* 8:28. doi:10.1186/1471-2156-8-28.

65. Zallen, J.A., Y. Cohen, A.M. Hudson, L. Cooley, E. Wieschaus, and E.D. Schejter. 2002. SCAR is a primary regulator of Arp2/3-dependent morphological events in Drosophila. *J. Cell Biol.* 156:689–701. doi:10.1083/jcb.200109057.

66. Zigmond, S.H., M. Evangelista, C. Boone, C. Yang, A.C. Dar, F. Sicheri, J. Forkey, M. Pring. 2003. Formin leaky cap allows elongation in the presence of tight capping proteins. *Curr. Biol.* 13(20):1820-3.

67. Zuchero, J.B., A.S. Coutts, M.E. Quinlan, N.B. La Thangue, and R.D. Mullins. 2009. p53-cofactor JMY is a multifunctional actin nucleation factor. *Nat. Cell Biol.* 11:451–

459. doi:10.1038/ncb1852.

68. Zuo, P., Z. Fu, T. Tao, F. Ye, L. Chen, X. Wang, W. Lu, and X. Xie. 2013. The expression of glia maturation factors and the effect of glia maturation factor-gamma on angiogenic sprouting in zebrafish. *Exp Cell Res*. 319:707–717. doi:S0014-4827(13)00007-4 [pii] 10.1016/j.yexcr.2013.01.004.

CHAPTER TWO: GMFB CONTROLS BRANCHED ACTIN CONTENT AND LAMELLIPODIAL RETRACTION IN FIBROBLASTS[1]

Introduction

Cell migration is fundamental to organismal development and survival, playing a critical role in processes ranging from neuronal development to wound healing. When cell migration goes awry, developmental defects and disease can occur. Problems in cell migration occur not only through failures in motility, but also through failure to recognize and respond to directional cues such as growth factors or extracellular matrix. Effective cell migration relies on proper regulation and coordination of actin networks. One such actin population is the branched actin network generated by the Arp2/3 complex (Pollard, 2007). Branched actin is found in the lamellipodium and is generated by activation of Arp2/3 by nucleation promoting factors (NPFs) like SCAR/WAVE and WASP (Rotty et al., 2013). Once active, Arp2/3 can nucleate a "daughter" filament at a characteristic angle of ~78° from the original "mother filament" (Rouiller et al., 2008).

The process of branched actin generation is well-studied, but less is known about how branched actin is disassembled. Coronin 1B was identified as having debranching activity through antagonizing the branch stabilizing protein cortactin, as well as destabilizing the

[1] Haynes, E. M, Asokan, S.B., King, S.J., Johnson, H.E., Haugh, J.M., Bear, J.E. 2015. GMFβ controls branched actin content and lamellipodial retraction in fibroblasts. *J. Cell. Biol.* 209(6):803-12. doi:10.1083/jcb.201501094.

branch itself (Cai et al., 2007, 2008). Coronin 1B has also been found to regulate ADF/cofilin activity at the leading edge via the slingshot phosphatase (Cai et al., 2007). Cofilin binds to actin filaments and severs them at low filament occupancy, but *in vitro* work shows that high occupancy of a filament by cofilin causes Arp2/3 debranching (Chan et al., 2009). Recently, the cofilin-related protein Glia Maturation Factor (GMF) has been implicated in Arp2/3 regulation (Lim et al., 1989; Gandhi et al., 2010; Ydenberg et al., 2013; Luan and Nolen, 2013).

Unlike cofilin, GMF has no actin binding or severing activity by *in vitro* assays (Gandhi et al., 2010; Nakano et al., 2010). However, addition of yeast GMF1 to pre-polymerized branched actin filaments resulted in debranching (Gandhi et al., 2010). At high concentrations GMF can also compete with NPFs for Arp2/3 complex binding, preventing branch formation (Gandhi et al., 2010; Nakano et al., 2010). This is thought to occur through one interface on GMF blocking the NPF WCA domain C-helix binding site on the Arp2/3 complex (Ydenberg et al., 2013; Luan and Nolen, 2013). A separate site on GMF is responsible for its debranching activity, which occurs through destabilization of the Arp2/3:daughter filament junction (Ydenberg et al., 2013; Luan and Nolen, 2013). Supporting its role in actin turnover, depletion of GMF has been associated with accumulation of actin patches in yeast and peripheral F-actin in *Drosophila* S2 cells and border cells (Nakano et al., 2010; Poukkula et al., 2014). Recent work in S2 cells shows that GMF localizes to the cell periphery, and its localization appears to increase upon retraction. Furthermore, border cells depleted of GMF have reduced protrusion dynamics early after detachment from the epithelium (Poukkula et al., 2014).

The two vertebrate GMF isoforms (GMFγ and GMFβ) are present in a variety of tissues. GMFγ is highly expressed in immune cells and vascular endothelium (Ikeda et al., 2006; Zuo et al., 2013), while GMFβ has high expression in the brain and is ubiquitously expressed in other tissues as revealed by RNAseq (Zuo et al., 2013; http://www.ebi.ac.uk/gxa/genes/ENSG00000197045). GMFγ has previously been implicated in leading edge dynamics, cell migration, and chemotaxis in multiple cell types (Ikeda et al., 2006; Aerbajinai et al., 2011; Lippert and Wilkins, 2012; Poukkula et al., 2014). Little work has been done on GMFβ, despite its homology to GMFγ. Here we provide a systematic analysis of how GMFβ affects branched actin, lamellipodial behavior and directional migration.

Results and Discussion

GMFβ displays Arp2/3-dependent localization to the leading edge

GMFβ was the only GMF isoform expressed in our IA32 mouse embryonic fibroblasts (Fig 2.S1 A), but both isoforms share considerable homology (Fig. 2.S1 B). Since yeast GMF1 and GMFγ are reported to bind to Arp2/3 complex, we reasoned that GMFβ should co-localize with branched actin at the leading edge. Indeed, GMFβ localized to lamellipodia when visualized by immunostaining for the endogenous protein (Fig. 2.1 A, top) or by expression of a GMFβ-GFP fusion (Fig. 2.1 A, bottom). This localization was lost in IA32 cells depleted of two subunits of the Arp2/3 complex, which lack lamellipodia (Fig 2.S1 C) (Wu et al., 2012). To ensure this localization was not an artifact of cell edge ruffling or increased volume at the cell edge, we used ratiometric imaging of cells expressing tRFP (a nonspecific volume marker) and either GFP alone, GMFβ-GFP or a GFP tagged subunit of Arp2/3 (p34-GFP). With this approach, GFP alone shows no specific edge localization (Fig.

2.1 B, left two panels; movie S1), whereas both GMFβ-GFP (Fig. 2.1 B, center; movie S1) and p34-GFP (Fig. 2.1 B, right; movie S1) show enhanced lamellipodial signal.

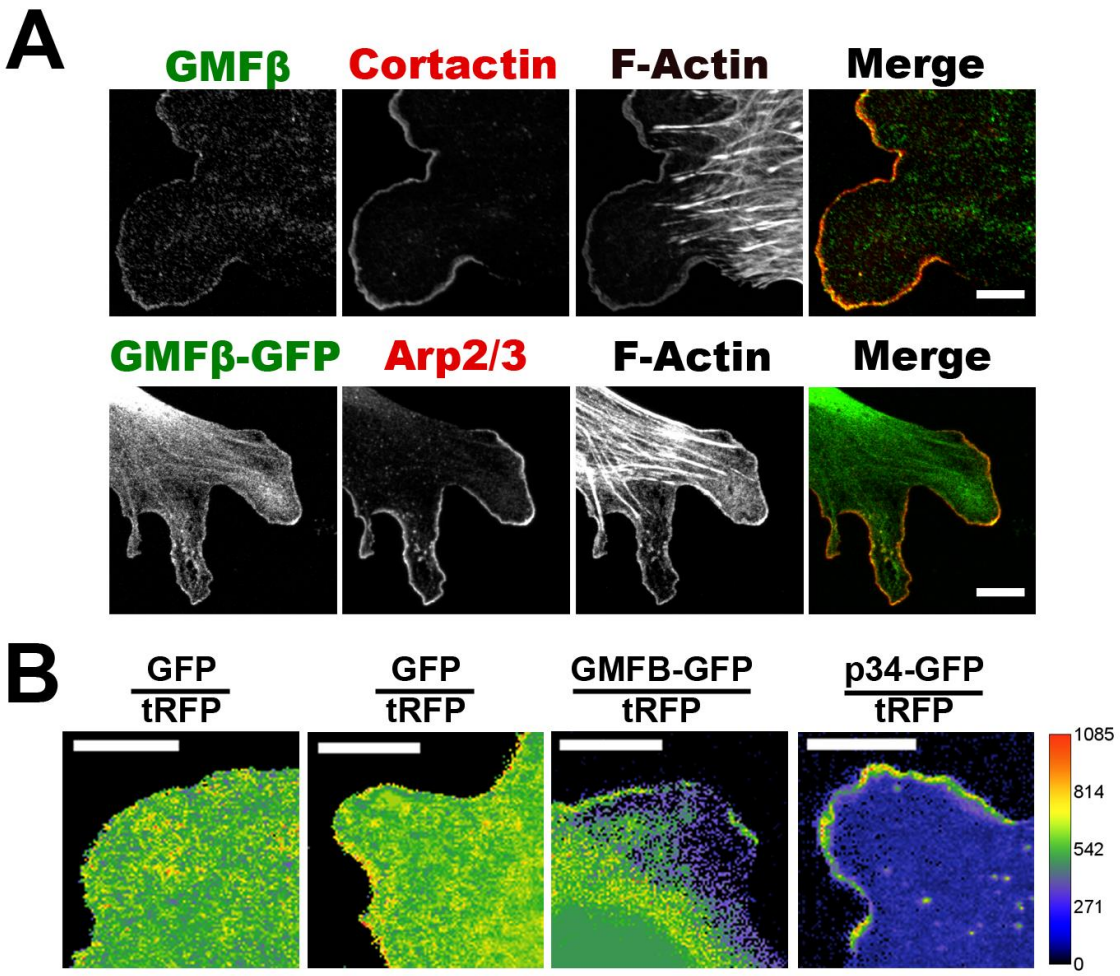

Figure 2.1 GMFβ localizes to the leading edge of fibroblasts.

A) GMFβ localization by immunofluorescence (IF) (top) and in cells expressing GMFβ-GFP (bottom). Arp2/3 or cortactin IF marks leading edge, bar = 10μm. **B)** Ratio of either soluble GFP, GMFβ-GFP, or p34-GFP to soluble RFP, bar = 10μm. Legend represents pixel intensity.

We suspected GMFβ may localize to lamellipodia only at specific times during their protrusion cycle, as GMFβ did not localize as uniformly as other leading edge markers (Fig. 2.1 B). To synchronize lamellipodia, we used the small molecule inhibitor of Arp2/3, CK-

666 (Nolen et al., 2009; Hetrick et al., 2013). Cells treated with CK-666 completely lost lamellipodia, which regrew in a synchronized manner upon drug washout (Fig. 2.S2 A). Cells remained primarily in the protrusion phase for 10 min post-washout, after which retraction and ruffling were observed (data not shown). Although cortactin returns to the lamellipodia within 1 min of CK-666 washout, GMFβ localization is delayed, appearing by 5 min post-washout (Fig. 2.2).

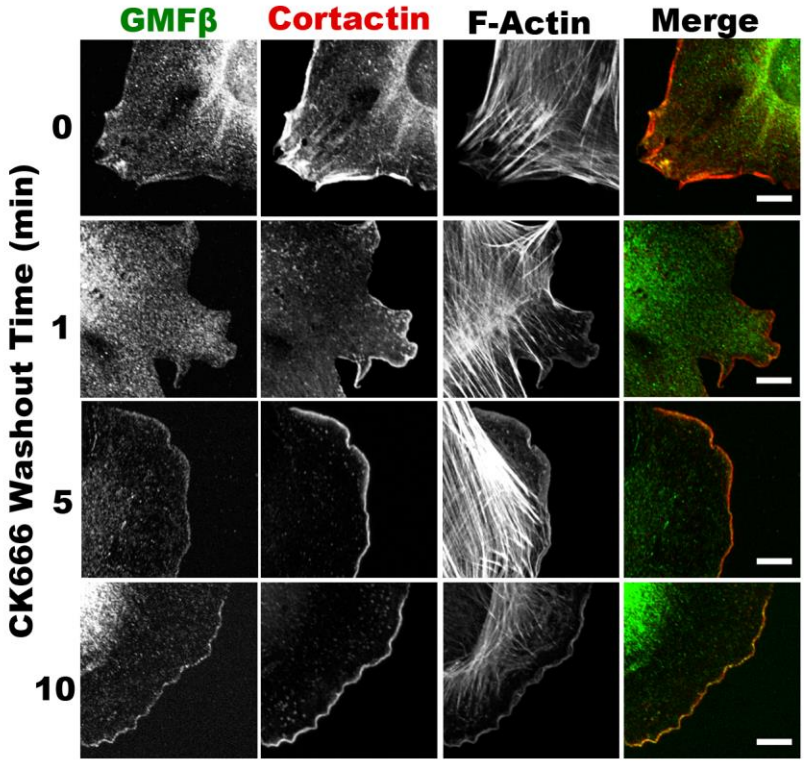

Figure 2.2 GMF localization is delayed in comparison to cortactin.

IF for GMFβ and cortactin of cells treated with CK-666 (150μM) to ablate lamellipodia, followed by washout for given times to allow lamellipodia regrowth, bar = 10μm.

GMFβ's delay in localization suggests that it does not affect the early protrusion phase, and that its localization may be dependent on the age of the branched actin network. This protrusion synchronization protocol was used in combination with contour-erosion based intensity measurements along the lamellipodia (Fig. 2.S1 D) to generate maps of the localization of either GMFβ-GFP or GFP alone after 10 minutes of CK-666 washout (Cai et al., 2007). While the maximum fluorescence intensity of GFP was measured towards the inside of cells (Fig. 2.S1 E), the maximum GMFβ-GFP fluorescence intensity occurred at the edge of cells in a similar pattern to Arp2/3 and actin (Fig. 2.S1 F). These data indicate that GMFβ edge localization is specific and dependent on the presence of Arp2/3-branched actin filaments.

GMFβ is critical for lamellipodial retraction

We next assessed GMFβ's role in lamellipodial dynamics. Using lentiviral expression of an shRNA for GMFβ, we created a GMFβ depleted cell line (KD), as well as a GMFβ depleted cell line rescued with an shRNA resistant GMFβ-GFP construct (KDR) (Fig. 2.3 A). GMFβ was barely detectable (<1%) by western blot after shRNA expression (Fig. 2.S1 G). An overexpression cell line (OE) was created by lentiviral infection of cells with a GMFβ-GFP construct followed by sorting for highly expressing cells (Fig. 2.3 B). The GMFβ depleted cell line displayed a larger spread size with broad lamellipodia in comparison to control cells (CNTL), which could be rescued by expressing shRNA-resistant GMFβ (KDR)

(Fig. 2.3 B; 2.4). Conversely, GMFβ overexpressing cells had lower spread area and smaller lamellipodia compared to control cells (Fig. 2.3 B; 2.4).

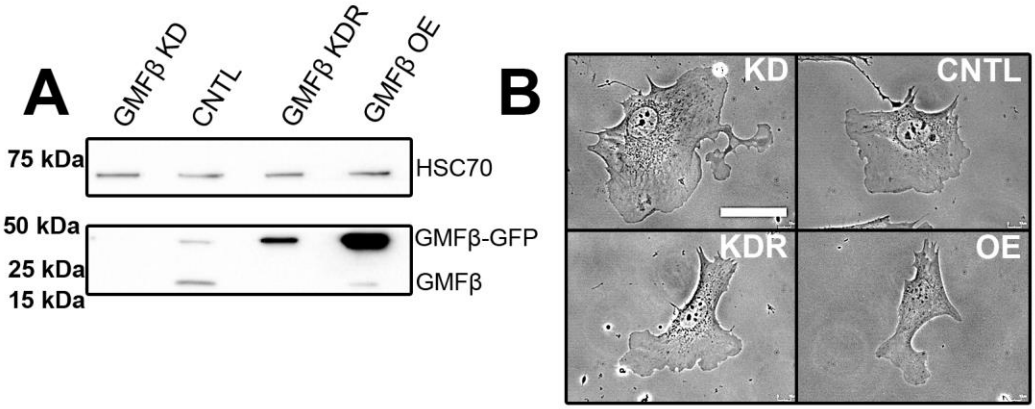

Figure 2.3 Modulating GMFβ causes phenotypic changes in cells.

A) Western blot showing GMFβ expression of created cell lines. **B)** GMFβ depleted (KD) and overexpressing (OE) cells show phenotypic changes vs control (CNTL) and knockdown-rescue (KDR) cell lines, bar = 50μm

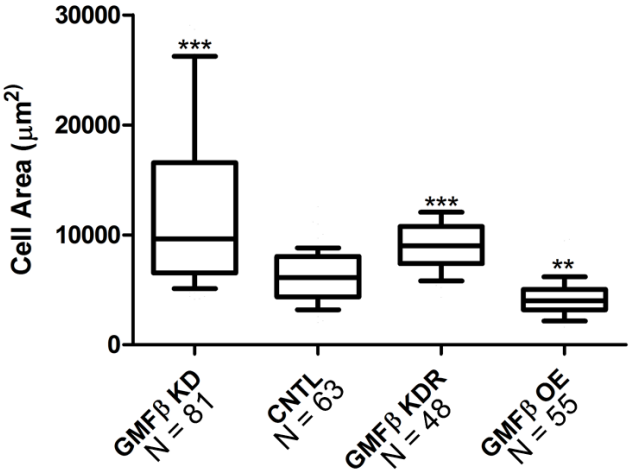

Figure 2.4 Cell area changes with GMFβ levels.

Cell area quantified from micrographs. Error bars represent 10th-90th percentile. Kruskal-Wallis multiple comparison testing was performed, and significance was measured by Dunn's post-test.($p<0.001$ = ***, $p < 0.01$ = **, $p <0.05$ = *)

These lamellipodia also behaved differently: GMFβ depleted cells had slower, less dynamic protrusions with little ruffling, while GMFβ overexpressing cells had dynamic protrusions with frequent ruffling. We analyzed cells by kymography, which confirmed our visual impressions (Fig. 2.5).

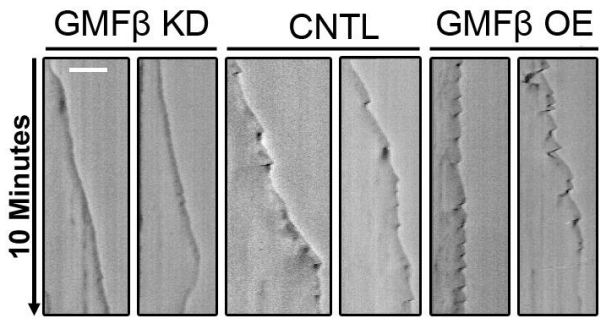

Figure 2.5 Example kymographs for GMFβ KD, CNTL, and GMFβ OE. Bar = 10μm.

GMFβ depleted cells had decreased protrusion rate and increased protrusion distance and duration (Fig. 2.6 A; 2.6 B; 2.6 C). More dramatically, depletion of GMFβ produced a severe reduction in retraction rate and frequency that could be rescued by re-expression of GMFβ (Fig. 2.6 D; 2.6 E). The observed increase in retraction and ruffling behavior in GMFβ overexpressing cells was not due to an actual increase in retraction frequency (Fig. 2.6 E) but instead due to an increase in the distance of each retraction event (Fig. 2.6 F). To summarize, GMFβ depleted cells retract slowly and less frequently, but for a longer total distance, while GMFβ overexpressing cells retract at the same speed and as frequently as control cells, but for an increased distance per retraction (Fig. 2.6 D; 2.6 E; 2.6 F).

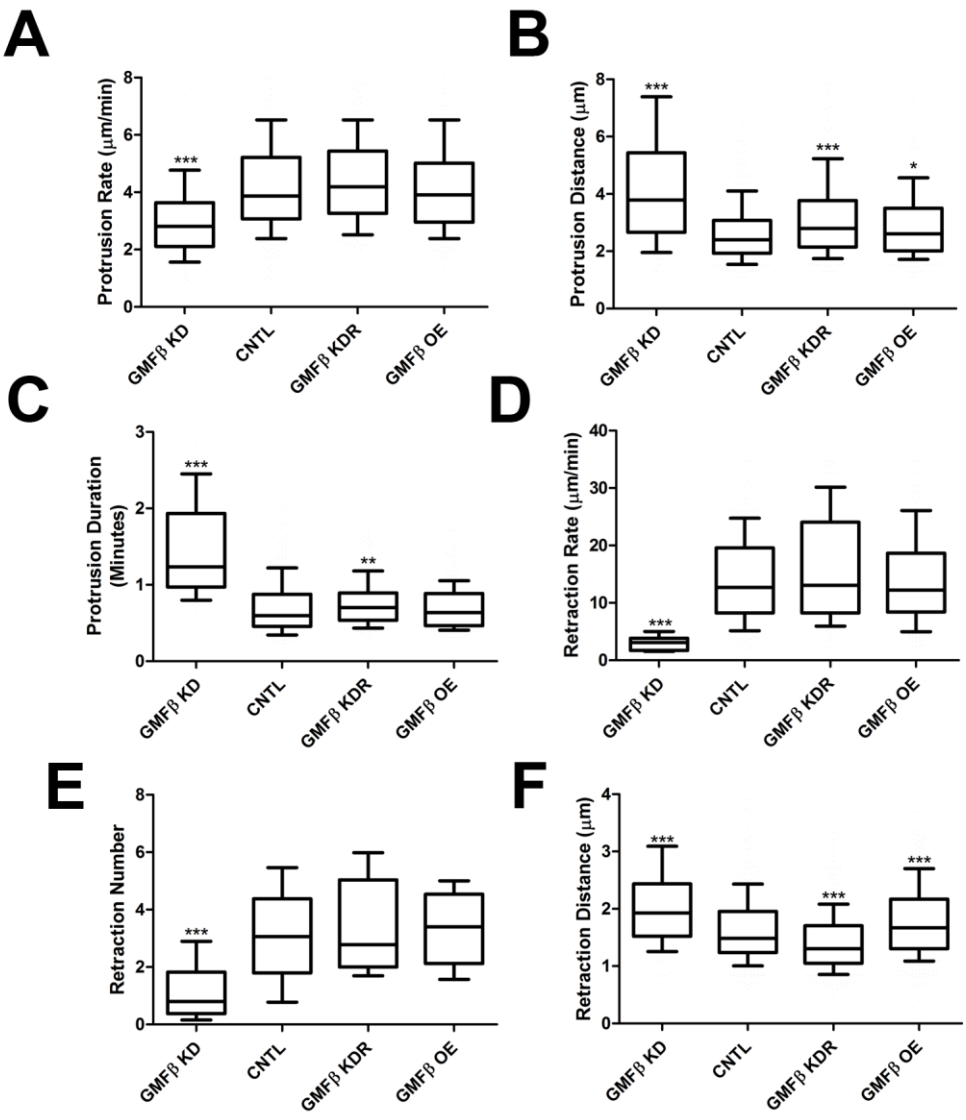

Figure 2.6 Lamellipodial dyanamics are controlled by GMFβ.

A) Protrusion rate in μm/min measured from kymography. **B)** Protrusion distance in μm. **C)** Protrusion duration in minutes. **D)** Retraction rate in μm/min. **E)** Average number of retractions per protrusion. **F)** Retraction length in μm. For all graphs, error bars represent 10th-90th percentile. Kruskal-Wallis multiple comparison testing was performed, and significance was measured by Dunn's post-test.($p<0.001$ = ***, $p < 0.01$ = **, $p <0.05$ = *) N>=20

Arp2/3 localization and stability is influenced by GMFβ

We next tested for changes to Arp2/3 complex content or dynamics by altering GMFβ expression. If GMFβ is 'pruning' Arp2/3-based branches, it is plausible that width or density (represented by Arp2/3 intensity) of lamellipodial branched actin could be altered by GMFβ depletion or overexpression. We used edge intensity mapping (Fig. 2.S1 D) to measure Arp2/3 complex intensity in protruding (synchronized) lamellipodia and in normally cycling (unsynchronized) lamellipodia. In synchronized populations there was no difference between GMFβ depleted cells and control cells in the front-to-back width or intensity of Arp2/3 complex (Fig. 2.7 A, left). However, overexpression of GMFβ greatly reduced the Arp2/3 complex intensity in synchronized cells (Fig. 2.7 A, right).

When the same analysis was performed on unsynchronized GMFβ depleted cells, an increase in the intensity of Arp2/3 complex at the cell edge was apparent, but the width of the branched actin network remained unchanged (Fig. 2.7 B, left). In unsynchronized GMFβ overexpressing cells, however, Arp2/3 intensity remained reduced as in synchronized populations (Fig. 2.7 B, right). Since synchronization of lamellipodia allows analysis of cells actively engaged in protrusion, our data suggest that GMFβ depleted cells generate branched actin similarly to control cells during this phase. In unsynchronized populations of lamellipodia, we are able to observe cells in mixed states of protrusion and retraction. Since GMFβ depleted cells have an increased accumulation of Arp2/3 complex in an unsynchronized state, this accumulation may be due to a defect in their retraction phase.

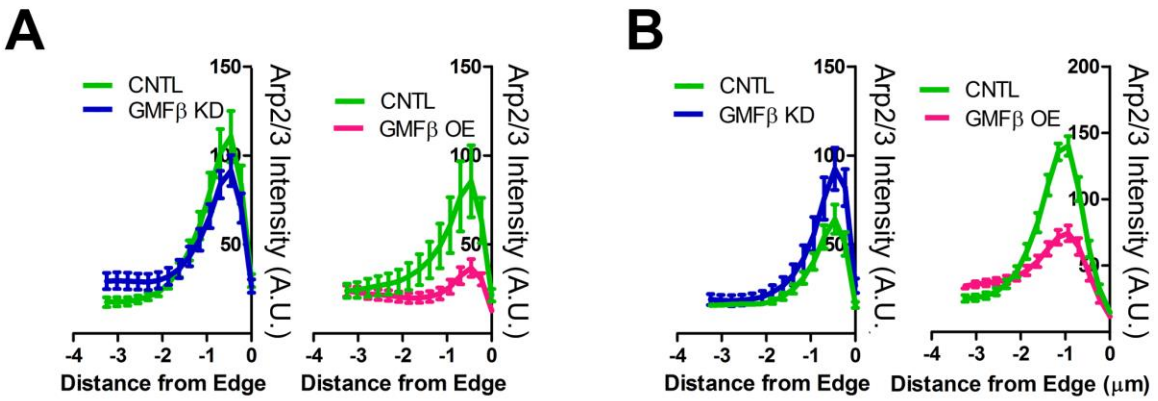

Figure 2.7 GMFβ controls the intensity of Arp2/3 at the leading edge of fibroblasts.

A) Mapping of p34 (Arp2/3) intensity in synchronized lamellipodia of GMFβ KD (left) or GMFβ OE (right) vs CNTL. Cell edge at 0. Error bars = SEM. **B)** Mapping of p34 (Arp2/3) intensity in unsynchronized lamellipodia of GMFβ KD (left) or GMFβ OE (right) vs CNTL, Cell edge at 0. Error bars = SEM.

Since we did not observe differences in the width of the branched actin network when GMFβ was depleted (despite visible differences in lamellipodia appearance and behavior), we hypothesized that GMFβ may instead control the distribution of Arp2/3 laterally. We immunostained synchronized cells to visualize the Arp2/3 complex (Fig. 2.8 A) and used a custom Matlab script to generate heatmaps of Arp2/3 along the cell edge (Fig. 2.8 A, insets) to determine the percent of the cell perimeter positive for Arp2/3 signal above the mean Arp2/3 intensity of the entire cell. Using this analysis we found that GMFβ depleted cells had an increase in Arp2/3-positive cell perimeter compared to control cells, while GMFβ overexpressing cells had reduced Arp2/3-positive cell perimeter (Fig. 2.8 B).

GMFβ is thought to have two branch antagonizing activities: directly destabilizing the existing branch junction, and preventing Arp2/3 activation by NPFs (Ydenberg et al., 2013; Luan and Nolen, 2013). The observed changes in Arp2/3 distribution could be due to either or both of these activities. If debranching is a main function of GMFβ, then depleting GMFβ

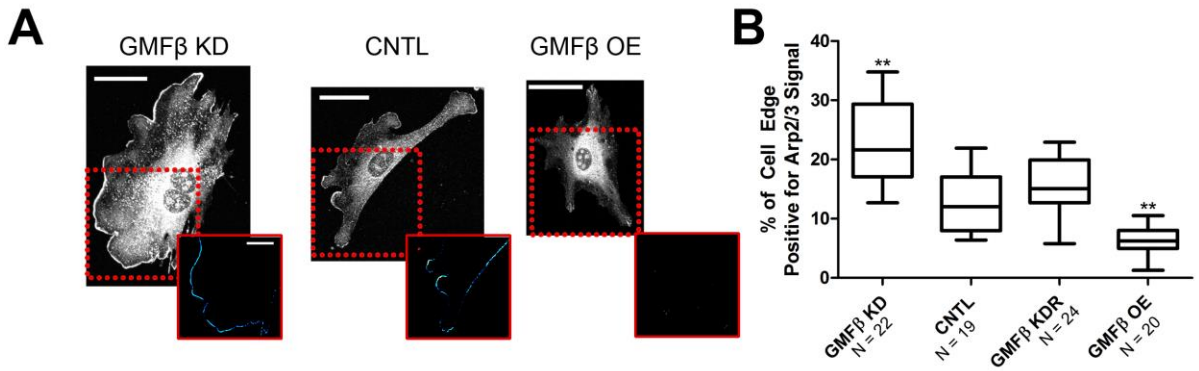

Figure 2.8 GMFβ influences the lateral spread of Arp2/3, and thus lamellipodia, around the cell.

A) Arp2/3 IF in GMFβ KD, CNTL, and GMFβ OE cells with synchronized lamellipodia. Bar = 50µm. Insets represent a computer-generated map of high Arp2/3 edge signal for each image, bar = 25µm. **B)** The percent of cell edge positive for high Arp2/3 signal, generated from p34 IF. Error bars represent 10th-90th percentile. Kruskal-Wallis multiple comparison testing was performed, and significance was measured by Dunn's post-test ($p<0.001$ = ***, $p < 0.01$ = **, $p <0.05$ = *)

should lead to observable changes in branched actin disassembly rate. To measure this, we used CK-666 wash-in to stop creation of new branches while leaving existing branches unaffected (Hetrick et al., 2013) (Fig. S1 H). Therefore, any decrease in Arp2/3 intensity at the leading edge represents the rate of branch disassembly. Using this technique in cells expressing a GFP tagged subunit of Arp2/3 (Wu et al., 2012), we observed an increase in the stability of the Arp2/3 complex upon GMFβ depletion (Fig. 2.9 A, movie S2). This could be observed by both measuring the amount of cell edge positive for Arp2/3 (Fig. 2.9 B) and the intensity of Arp2/3 signal at the edge (Fig. 2.9 C). While we cannot rule out NPF competition using this assay, it is notable that GMFβ overexpressing cells do not display a comparable phenotype to CK-666 treated cells. If GMFβ is blocking activation of Arp2/3 by NPFs, GMFβ overexpression should mimic inhibiting Arp2/3 by CK-666 treatment. While cells treated with CK-666 lose lamellipodia entirely and become dominated by bundled actin

structures (Fig. 2.S2 A), GMFβ overexpressing cells retain small dynamic lamellipodia with lower amounts of Arp2/3 complex (Fig. 2.S2 B). Furthermore, if GMFβ acts to suppress Arp2/3 activation, we should see an increase in intensity of Arp2/3 complex signal during the protrusion phase in synchronized GMFβ depleted cells (Fig 2.7 A, left). Instead, we only observed this increase in intensity when GMFβ depleted cells are unsynchronized (Fig 2.7 B, left). Together, these observations support debranching as the dominant role of GMFβ in our cells, and agree with recent studies *in vitro* showing that GMF had only weak inhibition of nucleation in the presence of the WCA domain of N-WASP, and no inhibition with the WCA domain of WAVE (Boczkowska et al., 2013).

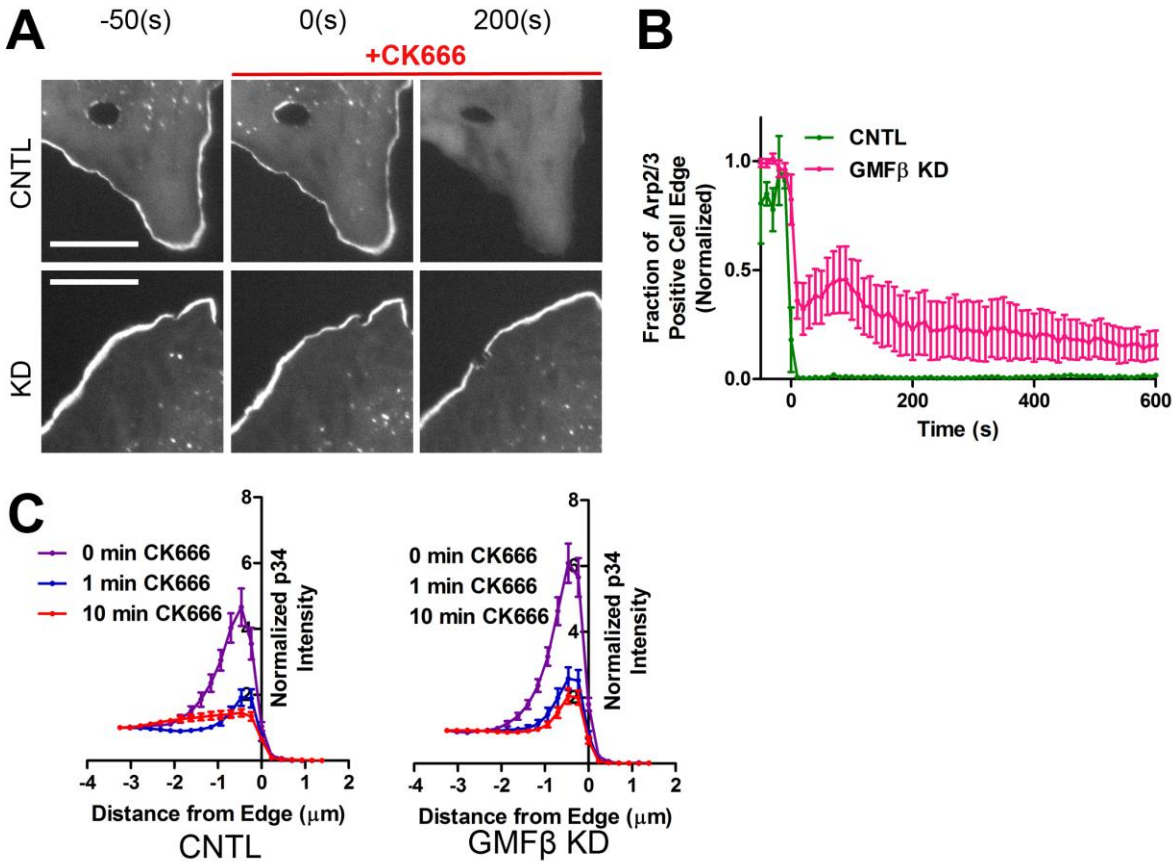

Figure 2.9 Depletion of GMFβ results in delayed loss of Arp2/3 signal from the leading edge after CK-666 treatment.

A) Stills from a live-cell wash-in of CK-666 on p34 knockdown cells rescued with p34-GFP (p34KDR). Control p34KDR cells (top) were compared to p34KDR cells depleted of GMFβ (bottom). CK-666 added at 0s, bar = 25μm. **B)** Representative movies from E were analyzed to determine the percentage of the cell edge occupied by high Arp2/3 signal. CNTL N = 3, GMFβ KD N = 5. Error bars = SEM. **C)** p34KDR WT and p34KDR cells depleted of GMFβ were treated with CK-666 for listed times and fixed, then edge intensity of p34-GFP was measured for each time point. Error bars = SEM. 0 min N = 16 for both CNTL and KD, all other times N = 14 cells for both CNTL and KD.

Mutant GMFβ cannot rescue GMFβ depletion phenotypes

Ydenberg et al created a series of mutations to assess which sites of budding yeast GMF1 were involved in debranching and NPF competition (Ydenberg et al., 2013). Two distinct sites were identified: site 1 appears required for NPF competition, while both sites 1

and 2 are for necessary for debranching. Thus a mutation affecting only debranching could be created. The mutation that caused the largest debranching defect in budding yeast GMF1 was also created in mouse GMFγ, where R19, K20, and R22 were changed to alanines and showed defective debranching activity (Ydenberg et al., 2013). We generated analogous mutations in GMFβ (R19A, K20A, R22A) to test if this mutant could rescue the defects observed in GMFβ depleted fibroblasts (Fig. 2.10). We found that this mutant GMFβ localized to the leading edge, although less robustly than wild type (WT) GMFβ-GFP (Fig. 2.11 A, 2.11 B). We created cell lines with mutant GMFβ which were comparable to our existing WT GMFβ cell lines. In addition to overexpressing mutant GMFβ in cells, a second cell line was made in which endogenous GMFβ was depleted by shRNA expression and cells were "rescued" with an shRNA resistant mutant GMFβ (Fig. 2.S2 C). We first compared the overexpression of the mutant GMFβ to the overexpression of WT GMFβ. In contrast to the overexpression of WT GMFβ, overexpression of mutant GMFβ increased cell size, reduced lamellipodial retraction rate, and increased Arp2/3 positive cell edge (Fig. 2.12 A; 2.12 C; 2.12 E). In the depletion-rescue experiment, expression of the mutant GMFβ construct did not rescue cell area, retraction rate, or percent of Arp2/3 positive cell edge (Fig. 2.12 B; 2.12 D; 2.12 F). Kymography of protrusion characteristics showed similar, but less pronounced trends in the mutant's inability to rescue depletion of endogenous GMFβ or mimic overexpression of WT GMFβ (Fig. 2.S2 D-I). This suggests that the debranching site of GMFβ is critical for its physiological role at the cell edge, and that defects in GMFβ depleted cells result from the loss of debranching activity.

Figure 2.10 Sequence alignment of GMF isoforms across species.

Human GMFβ (Hs) with *S. cerevisiae* (Sc), *Drosophila* (Dm) and *C. elegans (Ce)* GMF homologs. Mutated site indicated by red bracket.

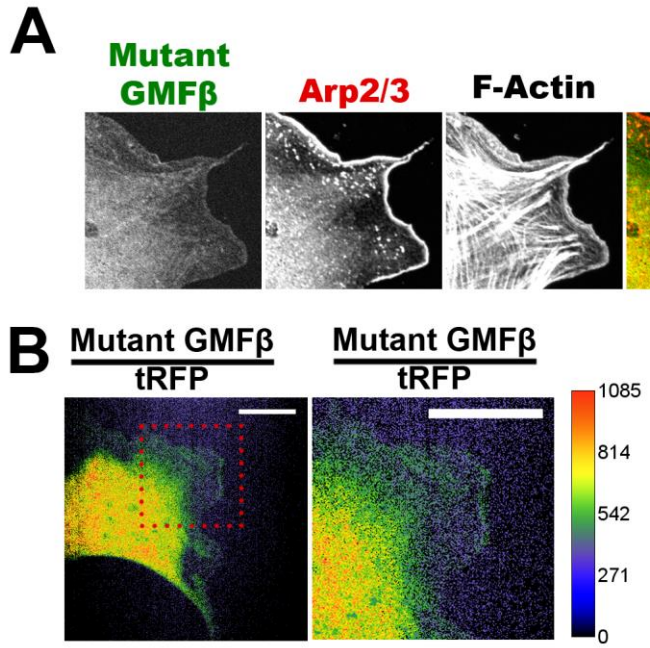

Figure 2.11 Mutant GMFβ localizes to the leading edge.

A) Localization of mutant GMFβ-GFP in unsynchronized cells. IF of Arp2/3 and F-actin, bar = 10μm **B)** Ratio of mutant GMFβ-GFP to soluble tRFP, bar = 25μm.

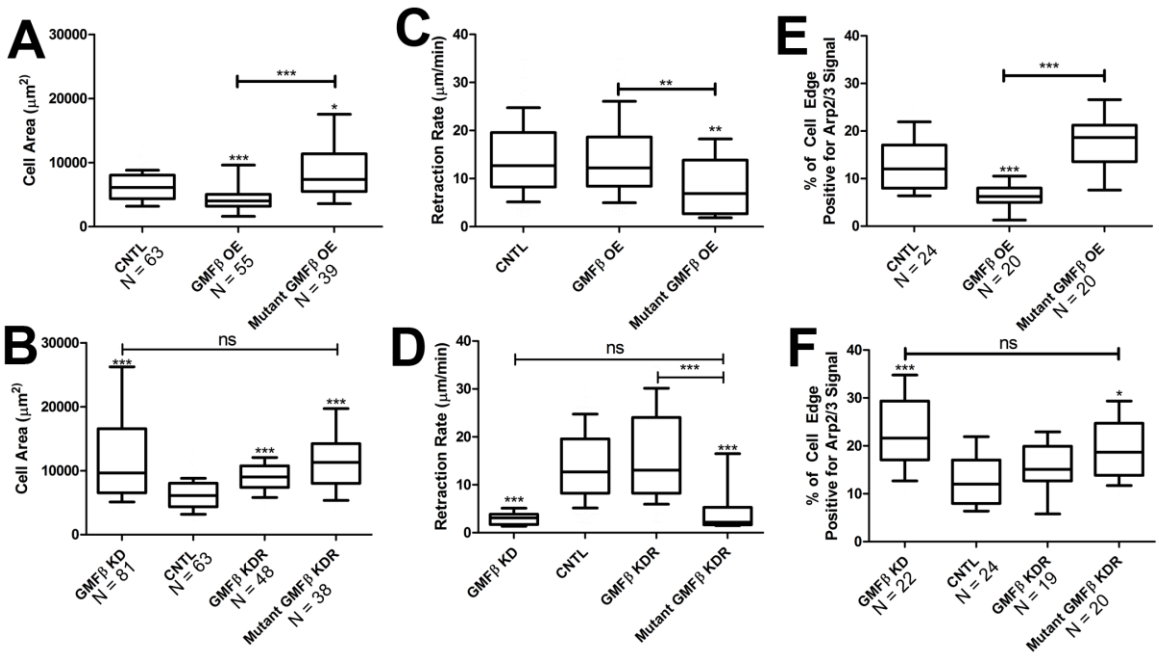

Figure 2.12 Mutant GMFβ cannot replicate GMFβ overexpression or rescue GMFβ depletion.

A) Cell area quantified from micrographs for mutant GMFβ OE **B)** Cell area quantified from micrographs for GMFβ KD cells rescued with mutant GMFβ (KDR). **C)** Retraction rate in μm/min for mutant GMFβ OE **D)** Retraction rate in μm/min for mutant GMFβ KDR **E)** The percent of cell edge positive for high Arp2/3 for mutant GMFβ OE **F)** The percent of cell edge positive for high Arp2/3 for mutant GMFβ KDR

For all graphs, error bars represent 10th-90th percentile. Kruskal-Wallis multiple comparison testing was performed, and significance was measured by Dunn's post-test ($p<0.001$ = ***, $p<0.01$ = **, $p<0.05$ = *)

Branched actin pruning by GMFβ is important for whole cell motility and is necessary for haptotaxis, but not chemotaxis

We sought to determine whether GMFβ related changes to lamellipodial dynamics affected whole cell migration. We found that depletion of GMFβ reduces cell velocity in single cell tracking assays of randomly migrating cells, while overexpression of GMFβ increases it (Fig. 2.13). These effects were not observed in Arp2/3 complex depleted cells, suggesting that GMFβ's effects on motility are Arp2/3-dependent (Fig. 2.S3 A). Re-

introduction of WT GMFβ into cells depleted of endogenous GMFβ rescued the observed defect in cell velocity (Fig. 2.13). Expression of mutant GMFβ, however, could neither rescue endogenous GMFβ depletion, nor replicate the overexpression phenotype of WT GMFβ (Fig 2.S3 B; 2.S3 C).

To address the role of GMFβ in directional migration, we used microfluidic chambers to generate gradients where cells can be directly observed during migration towards environmental cues (Wu et al., 2012; Asokan et al., 2014). Control cells plated within the same chambers served as internal controls for all experiments, and forward migration index (FMI) was used as a measure of directional motility (Asokan et al., 2014). A FMI with 95% confidence intervals (indicated by error bars) encompassing 0 represents inability to directionally migrate. We tested the ability of GMFβ overexpressing and GMFβ depleted cells to migrate towards soluble cues in the form of a gradient of PDGF (chemotaxis). Consistent with previous results that Arp2/3-based actin assembly is dispensable for PDGF chemotaxis in fibroblasts (Wu et al., 2012), both GMFβ overexpressing (Fig. 2.14 A) and GMFβ depleted (Fig. 2.14 B) cells could migrate up a concentration gradient of PDGF as well as control cells. Next, we assayed GMFβ's effect on cells migrating on a gradient of surface-bound extracellular matrix (haptotaxis). GMFβ overexpressing cells were unable to haptotax up a gradient of fibronectin in comparison to control cells (Fig. 2.15 A). Since GMFβ overexpressing cells have less Arp2/3 at the leading edge (Fig. 2.7 A, right), this result agrees with previous data from our lab showing that cells depleted of the Arp2/3 complex could not haptotax (Wu et al., 2012). However it is important to note that GMFβ overexpressing cells still have lamellipodia containing some Arp2/3, showing that less severe interruption of branched actin can abrogate haptotaxis (Fig. 2.S2 B). Cells depleted of GMFβ

were also unable to haptotax (Fig. 2.15 B), despite having an increase in both peak Arp2/3 edge intensity and percentage of Arp2/3 positive cell edge (Fig. 2.7 B; 2.8 B). Again, reintroduction of GMFβ-GFP into GMFβ depleted cells was able to rescue the defect in haptotaxis (Fig. 2.15 C). These data suggest that presence of lamellipodia is not sufficient for haptotaxis, and proper regulation of branched actin in the lamellipodia is critical for sensing and/or responding to an ECM gradient.

This study supports debranching by GMFβ as a prominent mechanism in the regulation of branched actin, allowing for appropriate lamellipodial retraction and limiting lateral lamellipodial growth. GMFβ does not appear to have significant effects on the protrusion phase of lamellipodial growth, where the effects of NPF competition should be most apparent. GMFβ likely acts in concert with other debranching and actin severing proteins (such as cofilin and coronins), as we observed a partial loss of Arp2/3 complex signal after CK-666 treatment in GMFβ-depleted cells (Fig. 2.9 C; 2.9 B). This implies that there may be a specific fraction of actin branches that GMFβ is crucial for pruning, but other debranching mechanisms may operate in parallel.

Our observations highlight the importance of the proper regulation of lamellipodia in controlling cell motility. Systems for reinforcing desired lamellipodia and eliminating unproductive lamellipodia are likely crucial for efficient management of actin within the cell and efficient cell migration. Moreover, our results reinforce the critical role that lamellipodia play in sensing and responding to ECM cues. One of the key unanswered questions arising from this work is how GMFβ might be regulated. Mechanisms that activate or inhibit GMFβ's activity would provide a potent way to regulate lamellipodial behavior and, ultimately, whole cell motility.

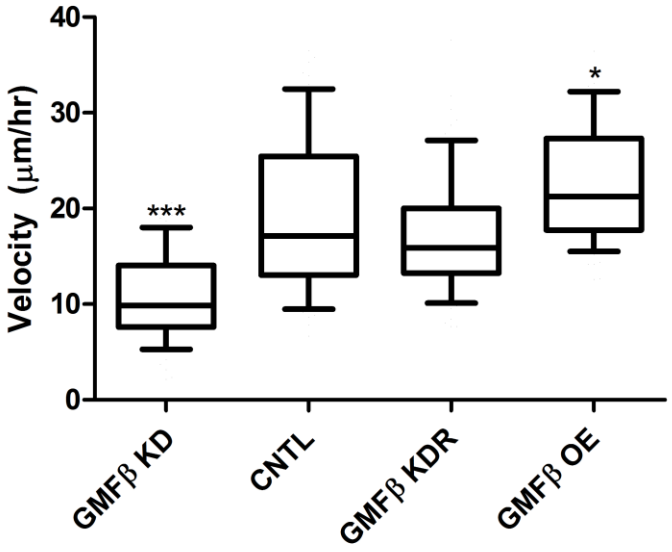

Figure 2.13 Random migration velocity is influenced by GMFβ expression levels.

Random migration velocity of single cells. Error bars represent 10th-90th percentile. N>60 for all conditions. Kruskal-Wallis multiple comparison testing was performed, and significance was measured by Dunn's post-test (p<0.001 = ***, p <0 .01 = **, p <0.05 = *)

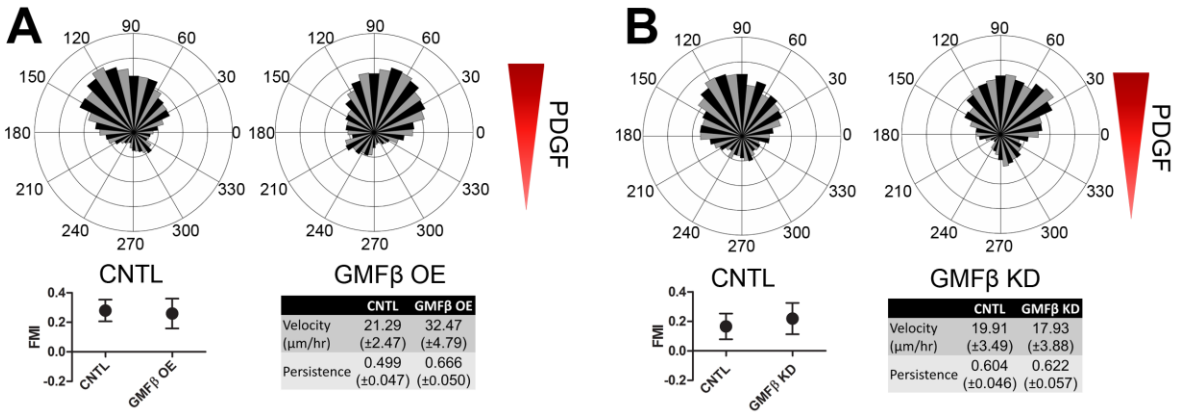

Figure 2.14 GMFβ has no effect on chemotaxis to PDGF.

A) Rose plots (top) for CNTL (left) and GMFβ OE (right) cells migrating in a PDGF gradient. Forward migration index (FMI) (bottom left), velocity and persistence (bottom right table) are provided. FMI plotted as the mean +/- the 95% confidence interval. Values in table

given as mean with 95% confidence interval. CNTL N = 89, OE N = 85. **B)** Rose plots (top) for CNTL (left) and GMFβ KD (right) cells migrating in a PDGF gradient. FMI, velocity, and persistence provided as previously. CNTL N = 118, KD N = 76.

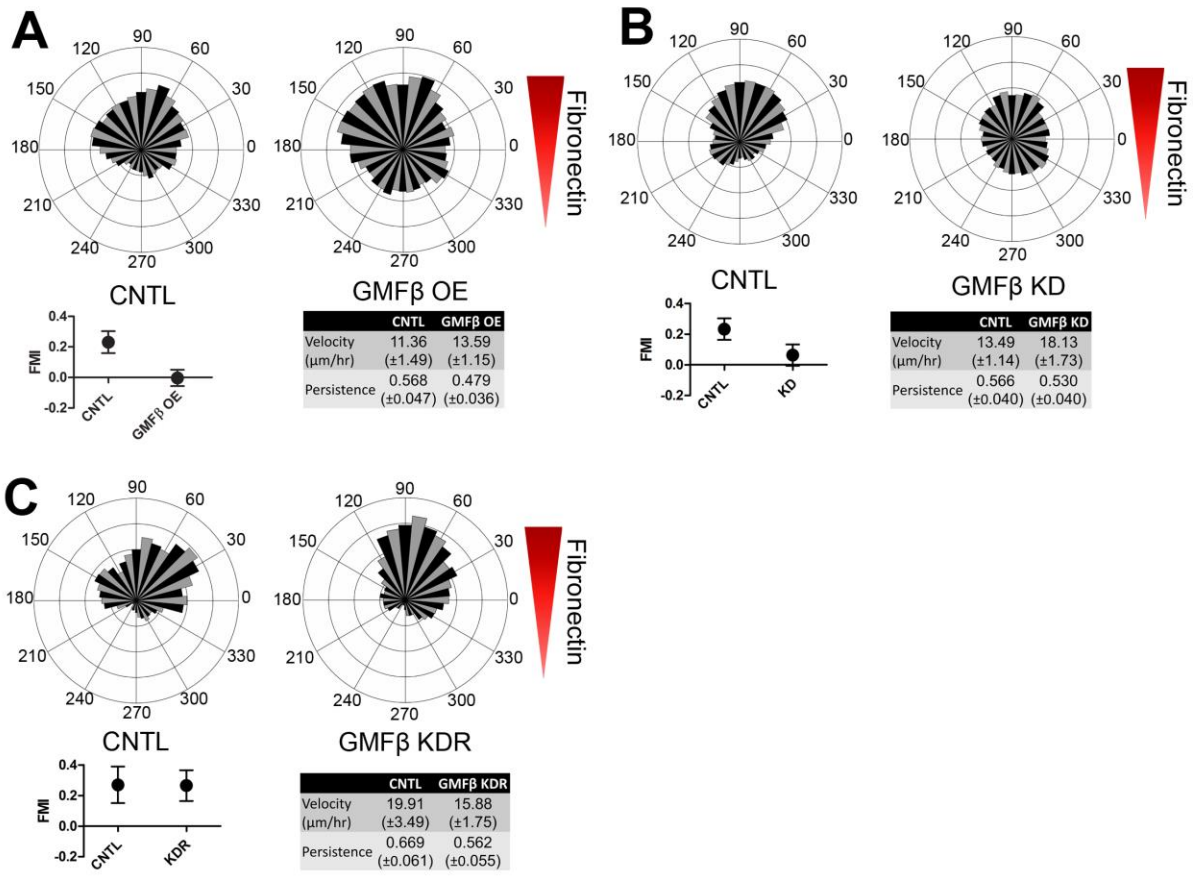

Figure 2.15 Disrupting normal GMFβ expression abrogates haptotaxis.

A) Rose plots (top) for CNTL (left) and GMFβ OE (right) cells migrating in a surface-bound fibronectin gradient. FMI, velocity, and persistence provided as previously. CNTL N= 130, OE N = 208. **B)** Rose plots (top) for CNTL (left) and GMFβ KD (right) cells migrating in a surface-bound fibronectin gradient. FMI, velocity, and persistence provided as previously. CNTL N = 144, KD N = 138. **C)** Rose plots (top) for CNTL (left) and GMFβ KDR (right) cells migrating in a surface-bound fibronectin gradient. FMI, velocity, and persistence plotted provided as previously. CNTL N = 41, KDR N = 59.

Materials and Methods

Reagents and Materials

Commercial antibodies were purchased from EMD Millipore (mouse anti-cortactin, rabbit anti-p34-Arc), Sigma-Aldrich (rabbit anti-GMFβ [SAB2701114, western blot and HPA002954, immunofluorescence]), Clontech (mouse anti-GFP), Santa Cruz (mouse anti-HSC70), Jackson Immunoresearch (HRP conjugated goat anti-mouse and goat anti-rabbit, Cy5, Cy2, and Rhodamine Red-X goat anti-rabbit, and Cy5 and Rhodamine Red-X goat anti-mouse secondary antibodies). Phalloidin was purchased from Life Technologies (Alexa Fluor 647, 568). Fibronectin for coating glass was purchased from BD Biosciences. The Arp2/3 inhibitor CK-666 was purchased from EMD Milipore. Transfections were performed with X-tremeGENE (Roche).

Plasmids

GMFβ shRNA plasmid (TRCN0000108774) from the UNC Chapel Hill Lenti-shRNA Core Facility, which uses the GE Healthcare TRC1 shRNA library. The hairpin sequence for this plasmid (5'-CCGG-CGAGCTAACCAAGGTATTTGA-CTCGAG-TCAAATACCTTGGTTAGCTCG-TTTTTG-3') is contained on the pLKO.1 vector and controlled by a human U6 promoter. The pLKO.1 puromycin resistance cassette is under the control of the hPGK promoter. GMFβ-GFP fusion constructs were made by PCR amplification of GMFβ from a GMFβ cDNA construct from the Human ORFeome (Internal ID: 5592), followed by cut-and-paste cloning into our pLL 5.0 and pLL 7.0 LentiLox plasmids, where the gene was controlled by a 5' UTR or CMV promoter, respectively. pLL5.0 was utilized for lower expressing cell lines (GMFβ KDR, mutant GMFβ) while pLL7.0 was utilized for overexpression. The mutant GMFβ construct was made by using

overlap extension PCR to introduce the R19, K20, and R22 mutations into the gene. The non-specific control hairpin target sequence is 5'-GATCGACTTACGACGTTAT-3', expressed in the pLL 5.0 plasmid. This sequence has no exact match in the human or mouse genome and has been previously characterized (Cai et al., 2007).

Cell Culture

Previously generated mouse embryonic fibroblast lines (IA32) from an Ink4a/Arf-/- background were used as our base cell line (Wu et al., 2012). 2xKD cells, which Wu et al generated by shRNA depletion of 2 subunits of Arp2/3 (p34Arc and Arp2) in IA32 cells, were also utilized (Fig S 1 C and Fig S 3 A). Cells were cultured in DMEM with 10% FBS, 100 U/ml penicillin, 100 µg/ml streptomycin, and 292 µg/ml l-glutamine. This media was also used for any live cell imaging performed.

Lentiviral infection and FACs sorting

Cell lines were generated by lentiviral infection using the pLL5.0 or pLL7.0 vectors as previously described (Cai et al., 2007). Briefly, the plasmid carrying the gene or shRNA of interest was co-transfected into Hek293-FT cells along with packaging vectors (Lois et al., 2002). Media is changed within 6-12 hours of transfection, and virus is collected after 2 days. The virus is spun down to remove cell debris and applied to cells for 2 days, then removed. Lentivirally infected cells expressing fluorescent protein were collected by fluorescence-activated cell sorting (FACS) with a Bio-Rad S3 Cell Sorter into desired populations (top 10% for GMFβ overexpressing cells, bottom 10% for cells used to make GMFβ KDR, all other lines sorted for all positive). Lentivirally infected cells expressing shRNA for GMFβ were selected by puromycin for 2 days at 2µg/ml before use in assays. Control (CNTL) cells used in comparison with GMFβ shRNA knockdown lines were IA32 cells infected with a

non-specific shRNA hairpin and expressing a GFP marker. These cells were also used as control cells used in comparison with GMFβ overexpressing lines in experiments where both GMFβ knockdown lines and overexpressing lines were being directly compared. Uninfected wild type IA32 cells were used as a control for GMFβ overexpressing cells in experiments where GMFβ depleted and GMFβ overexpressing cells were not being directly compared (Fig. 2.3 A, right, 2.3 B, right, and Fig. 2.5 B and D).

Western Blotting

Western blotting performed in accordance with standard technique (Rotty et al. 2014). Cells plated 70-80% confluent were washed with PBS and lysed by scraping with 4°C RIPA buffer containing protease inhibitors (1,10 phenenthroline and aprotinin, Sigma. Leupeptin, Roche.). Blots for GMFβ were blocked in a mixture of 5% milk and 5% BSA to reduce background. Rabbit anti-GMFβ antibody (Sigma) was used at a 1:750 dilution and incubated overnight at 4°C. Blots were imaged using a ChemiDoc MP (Bio-Rad) and analyzed using ImageLab 5.0. Representative blots are shown out of a set of at least 3 independent experiments.

Microscopy and Image Analysis

Immunofluorescence and Lamellipodial Synchronization

Cells were plated on coverslips coated with 10 µg/ml fibronectin and left to spread overnight before being either fixed with 4°C 4% PFA in Krebs-S Buffer (for unsynchronized populations) or treated to synchronize lamellipodia. Lamellipodial synchronization was achieved by addition of 150µM CK-666 for 2 hours, followed by washout of the drug with regular DMEM for 10 minutes (unless otherwise specified) before fixation. Cells were then

permeabilized in 0.1% Triton-X100 for 5 minutes. 5% BSA/NGS mixture was used to block for 1 hour. Primary antibody was added either 4°C overnight or 2 hours at room temperature. Secondary antibody was added for 1.5 hours at room temperature. Coverslips were washed thoroughly with PBS and then mounted using Fluoromount-G (Electron Microscopy Sciences) or Fluorogel with Tris buffer (Electron Microscopy Sciences). In comparative experiments, control and test cells were plated in mixed populations on the same coverslip and GFP expression or Cell Tracker dyes (Life Technologies) were used to identify populations. Coverslips were imaged on an Olympus FV1000 or FV1200 confocal microscope with a Hamamatsu PMT controlled by Fluoview with a 40x 1.3 NA Olympus objective at room temperature. Micrographs are displayed as maximum intensity projections of z-stacks.

Ratio Imaging

Cells stably expressing tagRFP-t were co-infected with either soluble GFP, GMFβ-GFP, Mutant GMFβ-GFP or p43-GFP. Cells were imaged on a Zeiss 5-Live confocal with a humidified environmental chamber (37°C, 5% CO_2) using a 63x 1.4 NA Zeiss objective and LSM DuoScan controlled by LSM 5 software. Cells were imaged at 10 second intervals for 20 minutes. These movies were analyzed in imageJ using the image calculator. The target of interest was set as the numerator, and the control protein (tagRFP-t) was set as the denominator. The resulting ratio image was then multiplied by a mask of the thresholded denominator to reduce background noise.

Edge Mapping Analysis

Edge mapping of leading edge proteins was performed using the ImageJ macro "Edgeratio" (Cai et al., 2007). Briefly, maximum intensity projections were generated from

confocal images of cells, and the projection for each channel imaged was combined into an RGB image. Regions which were positive for p34 (Arp2/3) or cortactin staining were considered lamellipodia and selected for analysis by a hand-drawn mask (Fig 2.S1 D). A threshold is generated to select the entire cell, and this selection is eroded or expanded to obtain average intensity values along the edge at various distances from the cell edge for each channel (Figure 2.S1 D). For GMFβ-GFP localization data, cells were unsynchronized and the signal was normalized to the peak fluorescence signal in the cell. Arp2/3 leading edge intensity measurements were performed on either p34 knockdown cells rescued with p34-GFP (p34-KDR) (for GMFβ KD cells and their respective controls), or anti-p34 immunostaining (for GMFβ OE cells and their respective controls). Arp2/3 (p34) intensity was presented raw and without normalization.

Kymography and Random Cell Migration

Cells were plated overnight on glass bottomed Mat-TEK dishes coated with 10 μg/mL fibronectin. Cells used for kymography were imaged on a Nikon Biostation IM at 40x using 2 second intervals for 10 minutes. Kymographs were created from movies in ImageJ using the Kymograph plugin (http://www.embl.de/eamnet/html/body_kymograph.html). Lines were drawn along protrusions and retractions, and the angles and lengths of these lines were recorded. A perl script was used to analyze the data and output protrusion rates, etc. Random cell migration was also performed on the Biostation IM using the 20x objective. Cells were imaged for 12 hours and then tracked using the Manual Tracking plugin for ImageJ (http://rsbweb.nih.gov/ij/plugins/track/track.html).

Cell Size Analysis

Phase micrographs of unsynchronized cells were manually outlined in ImageJ and the "measure" function was used to output the total cell area in μm^2.

CK-666 Wash-in

p34-KDR cells were plated overnight in 8 well chamber slides (Nunc) coated with 10 μg/mL fibronectin. Holes were punched through the lid of the chamber slide to allow tubing to be inserted, and this was connected to a syringe filled with CK-666 at 300μM. An equal volume of CK-666 containing media was washed in to the existing media in the well to achieve a final concentration of 150μM. Cells were imaged with epifluorescence in a humidified environmental chamber (37° C, 5% CO_2) on an Olympus IX81 microscope using a 60x 1.49 NA objective and Hamamatsu Orca-ER camera controlled by Metamorph. Images were captured at 5 second intervals as drug was applied, and imaging continued for at least 20 minutes after addition. The resulting live cell movies were analyzed for percentage of Arp2/3 complex positive edge, as described below. Since this experiment only allowed us to image a single cell at a time, we also performed a CK-666 wash-in on p34-KDR cells plated on fibronectin coated coverslips. These cells were treated with CK-666 containing media for 1 or 10 minute(s) and then fixed immediately. Cells were stained with anti-GFP antibody, mounted, and imaged via confocal as described previously. p34-GFP intensity was measured from these images using the Edgeratio macro and normalized to the first datapoint (at -3.25 μm from the edge).

Percentage of Arp2/3 Complex Positive Edge Analysis

Maximum intensity projections of synchronized cells immunostained for the p34 subunit of the Arp2/3 complex were generated as described, and these images were analyzed using a Matlab (Mathworks) program. K-means clustering was used to automatically segment the cell. A 10-pixel ring around the cell perimeter was defined, and the Arp2/3 signal at least 0.8 standard deviations above the mean was detected. The amount of cell edge marked by this high Arp2/3 signal was divided by the total perimeter of the cell, then multiplied by 100 to calculate the percentage of Arp2/3 positive cell edge.

Directional Migration Assays

Directional migration assays were performed as previously described (Wu et al., 2012, 2013). Briefly, PDMS chambers containing microcapillaries were used to establish a gradient by flowing attractant in the source chamber, and a neutral media in the sink chamber. A constant flow of PDGF was used for the chemotactic gradient, while a fibronectin gradient was established for haptotaxis. Control and test cells were plated together in the central chamber containing the gradient, and GFP expression or cell dyes were used to distinguish populations. For chemotaxis experiments, cells were imaged for 24 hours using a 20x Olympus objective on an Olympus inverted microscope (IX81) with a humidified environmental chamber (37°C, 5% CO_2) and Hamamatsu Orca-ER camera controlled by Metamorph. For haptotaxis experiments, cells were imaged for 16 hours on the Olympus Vivaview incubator microscope system (humidified, 37°C, 5% CO_2) using a 20x .75 NA objective with magnification set to 0.5x, which was controlled by Metamorph. Cells were tracked using the "Manual Tracking" plugin for ImageJ and these tracks were analyzed with the Chemotaxis Tool plugin from Ibidi to obtain forward migration index, persistence,

and velocity measurements. Rose plots were generated using the secplot script for Matlab (http://www.mathworks.com/matlabcentral/fileexchange/14174-secplot).

Statistical Analysis

All statistical analysis on generated data was performed using the software Prism (GraphPad). Error bars on boxplots represent the 10^{th}-90^{th} percentiles. Error bars on XY plots represent the standard error of the mean. Error bars on forward migration index plots represent the 95% confidence intervals. Box plot data was analyzed using the Kruskal-Wallis test to determine that individual samples did not come from identical populations. Statistical significance was determined by Dunn's post-test after the Kruskal-Wallis test was performed.

REFERENCES

1. Aerbajinai, W., L.H. Liu, K. Chin, J.Q. Zhu, C.A. Parent, and G.P. Rodgers. 2011. Glia maturation factor-gamma mediates neutrophil chemotaxis. *J. Leukoc. Biol.* 90:529–538. doi:Doi 10.1189/Jlb.0710424.

2. Asokan, S.B., H.E. Johnson, A. Rahman, S.J. King, J.D. Rotty, I.P. Lebedeva, J.M. Haugh, and J.E. Bear. 2014. Mesenchymal Chemotaxis Requires Selective Inactivation of Myosin II at the Leading Edge via a Noncanonical PLCγ/PKCα Pathway. *Dev. Cell*. 31:747–760. doi:http://dx.doi.org/10.1016/j.devcel.2014.10.024.

3. Cai, L., A.M. Makhov, D.A. Schafer, and J.E. Bear. 2008. Coronin 1B antagonizes Cortactin and remodels Arp2/3-containing actin branches in lamellipodia. *Cell*. 134:828–842. doi:10.1016/j.cell.2008.06.054.

4. Cai, L., T.W. Marshall, A.C. Uetrecht, D.A. Schafer, and J.E. Bear. 2007. Coronin 1B coordinates Arp2/3 complex and Cofilin activities at the leading edge. *Cell*. 128:915–929. doi:10.1016/j.cell.2007.01.031.

5. Chan, C., C.C. Beltzner, and T.D. Pollard. 2009. Cofilin Dissociates Arp2/3 Complex and Branches from Actin Filaments. *Curr. Biol.* 19:537–545. doi:10.1016/j.cub.2009.02.060.

6. Gandhi, M., B.A. Smith, M. Bovellan, V. Paavilainen, K. Daugherty-Clarke, J. Gelles, P. Lappalainen, and B.L. Goode. 2010. GMF is a cofilin homologue that binds Arp2/3 complex to stimulate filament debranching and inhibit actin nucleation. *Curr. Biol.* 20:861–867. doi:10.1016/j.cub.2010.03.026.

7. Hetrick, B., M.S. Han, L.A. Helgeson, and B.J. Nolen. 2013. Small molecules CK-666 and CK-869 inhibit actin-related protein 2/3 complex by blocking an activating conformational change. *Chem Biol*. 20:701–712. doi:S1074-5521(13)00124-5 [pii] 10.1016/j.chembiol.2013.03.019.

8. Ikeda, K., R.K. Kundu, S. Ikeda, M. Kobara, H. Matsubara, and T. Quertermous. 2006. Glia maturation factor-gamma is preferentially expressed in microvascular endothelial and inflammatory cells and modulates actin cytoskeleton reorganization. *Circ Res*. 99:424–433. doi:01.RES.0000237662.23539.0b [pii] 10.1161/01.RES.0000237662.23539.0b.

9. Lim, R., J.F. Miller, and A. Zaheer. 1989. Purification and characterization of glia maturation factor beta: a growth regulator for neurons and glia. *Proc. Natl. Acad. Sci. U. S. A.* 86:3901–3905.

10. Lippert, D.N., and J.A. Wilkins. 2012. Glia maturation factor gamma regulates the migration and adherence of human T lymphocytes. *BMC Immunol*. 13:21. doi:1471-

2172-13-21 [pii] 10.1186/1471-2172-13-21.

11. Lois, C., E.J. Hong, S. Pease, E.J. Brown, and D. Baltimore. 2002. Germline Transmission and Tissue-Specific Expression of Transgenes Delivered by Lentiviral Vectors. *Sci.* . 295 :868–872. doi:10.1126/science.1067081 .

12. Luan, Q., and B.J. Nolen. 2013. Structural basis for regulation of Arp2/3 complex by GMF. *Nat. Struct. Mol. Biol.* 20:1062–1068. doi:10.1038/nsmb.2628.

13. Nakano, K., H. Kuwayama, M. Kawasaki, O. Numata, and M. Takaine. 2010. GMF is an evolutionarily developed Adf/cofilin-super family protein involved in the Arp2/3 complex-mediated organization of the actin cytoskeleton. *Cytoskelet.* 67:373–382. doi:10.1002/cm.20451.

14. Nolen, B.J., N. Tomasevic, A. Russell, D.W. Pierce, Z. Jia, C.D. McCormick, J. Hartman, R. Sakowicz, and T.D. Pollard. 2009. Characterization of two classes of small molecule inhibitors of Arp2/3 complex. *Nature*. 460:1031–1034. doi:nature08231 [pii] 10.1038/nature08231.

15. Pollard, T.D. 2007. Regulation of Actin Filament Assembly by Arp2/3 Complex and Formins. *Annu. Rev. Biophys. Biomol. Struct.* 36:451–477. doi:10.1146/annurev.biophys.35.040405.101936.

16. Poukkula, M., M. Hakala, N. Pentinmikko, M.O. Sweeney, S. Jansen, J. Mattila, V. Hietakangas, B.L. Goode, and P. Lappalainen. 2014. GMF Promotes Leading-Edge Dynamics and Collective Cell Migration In Vivo. *Curr Biol*. 24:2533–2540. doi:S0960-9822(14)01130-0 [pii] 10.1016/j.cub.2014.08.066.

17. Rotty, J.D., C. Wu, and J.E. Bear. 2013. New insights into the regulation and cellular functions of the ARP2/3 complex. *Nat Rev Mol Cell Biol*. 14:7–12.

18. Rotty, J.D., C. Wu, E.M. Haynes, C. Suarez, J.D. Winkelman, H.E. Johnson, J.M. Haugh, D.R. Kovar, and J.E. Bear. Profilin-1 Serves as a Gatekeeper for Actin Assembly by Arp2/3-Dependent and -Independent Pathways. *Dev. Cell*. doi:http://dx.doi.org/10.1016/j.devcel.2014.10.026.

19. Rouiller, I., X.-P. Xu, K.J. Amann, C. Egile, S. Nickell, D. Nicastro, R. Li, T.D. Pollard, N. Volkmann, and D. Hanein. 2008. The structural basis of actin filament branching by the Arp2/3 complex. *J. Cell Biol.* . 180 :887–895. doi:10.1083/jcb.200709092.

20. Wu, C., S.B. Asokan, M.E. Berginski, E.M. Haynes, N.E. Sharpless, J.D. Griffith, S.M. Gomez, and J.E. Bear. 2012. Arp2/3 is critical for lamellipodia and response to extracellular matrix cues but is dispensable for chemotaxis. *Cell*. 148:973–987.

21. Wu, C., E.M. Haynes, S.B. Asokan, J.M. Simon, N.E. Sharpless, A.S. Baldwin, I.J. Davis, G.L. Johnson, and J.E. Bear. 2013. Loss of Arp2/3 induces an NF-κB-dependent, nonautonomous effect on chemotactic signaling. *J. Cell Biol.* 203:907–916.

22. Ydenberg, C.A., S.B. Padrick, M.O. Sweeney, M. Gandhi, O. Sokolova, and B.L. Goode. 2013. GMF severs actin-Arp2/3 complex branch junctions by a cofilin-like mechanism. *Curr. Biol.* 23:1037–1045. doi:10.1016/j.cub.2013.04.058.

23. Zuo, P., Z. Fu, T. Tao, F. Ye, L. Chen, X. Wang, W. Lu, and X. Xie. 2013. The expression of glia maturation factors and the effect of glia maturation factor-gamma on angiogenic sprouting in zebrafish. *Exp Cell Res*. 319:707–717. doi:S0014-4827(13)00007-4 [pii] 10.1016/j.yexcr.2013.01.004.

Supplemental Data

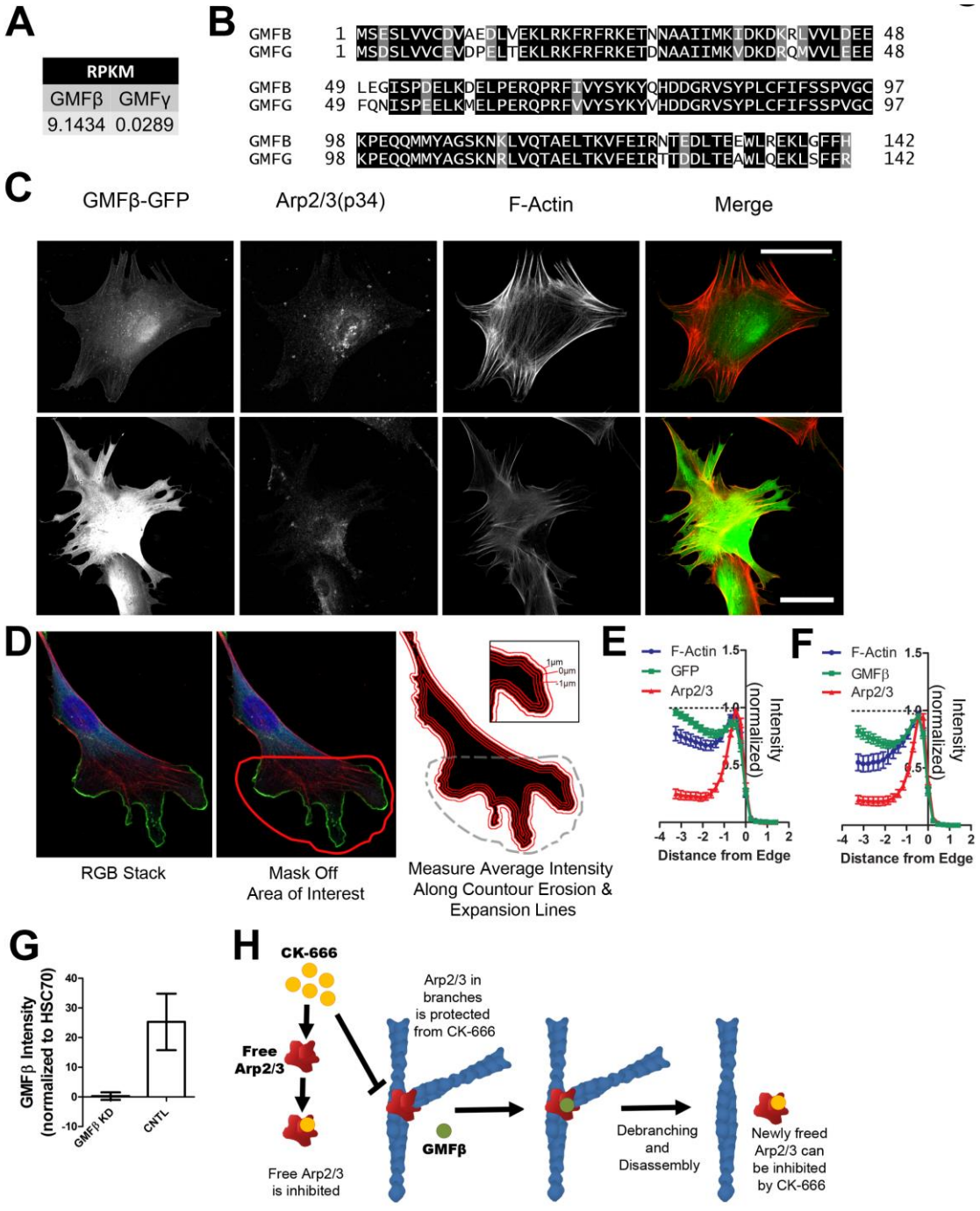

Supplemental Figure 2.1 GMFβ but not GMFγ is expressed in fibroblasts and localizes specifically to the leading edge. CK-666, a small molecular inhibitor of Arp2/3, can be used to provide insights on Arp2/3. Related to figures 1 and 3.

(A) GMFβ vs GMFγ expression in our mouse embryonic fibroblast line as measured by RNA-seq analysis. RPKM = Reads Per Kilobase of transcript per Million mapped reads.

(B) Sequence alignment of human GMFβ (GMFB) with human GMFγ (GMFG).

(C) Cells depleted of 2 subunits of Arp2/3 (p34Arc and Arp2) have no lamellipodia and do not display GMFβ-GFP localization at the cell edge. 50 μm scale bar.

(D) Example of contour erosion line scans (right) generated from a fluorescent image of a cell (left). The edge of the cell is detected using an ImageJ macro and line scans for a user-defined area of the cells (such as the lamellipodia) are generated automatically at various distances from the cell edge. Here, example contour lines are drawn at 1μm intervals. The average fluorescence intensity for the lines inside the defined region is recorded and plotted.

(E) Edge intensity map generated for GFP expressing cells. Fluorescence for each channel is normalized to the highest intensity value for that channel in the entire cell. GFP reaches peak fluorescence intensity towards the inside of the cell, away from the leading edge marker Arp2/3.

(F) Edge intensity map generated for GMFβ-GFP expressing cells. GMFβ-GFP reaches peak fluorescence intensity at the cell edge, comparable to Arp2/3.

(G) Quantification of GMFβ knockdown via western blot of lysates from 4 separate experiments. GMFβ intensity and HSC70 (control) intensity was measured with local background subtracted, then the GMFβ signal was divided by the HSC70 signal to normalize.

(H) The CK-666 Wash-in experiment: when 150μM CK-666 is added to cells, Arp2/3 which is not occupied in branches is bound by CK-666 and inactivated, preventing new branch formation. Arp2/3 which is currently in branches is protected from CK-666, until it is turned over by debranching or disassembly (for example, by GMFβ). Once Arp2/3 is removed from the branch and becomes free again, CK-666 can bind it and block its incorporation into new branches. Therefore, using this assay, the disappearance of Arp2/3 from the leading edge should reflect the disassembly rate of the branch network without any confounding effects of branch creation.

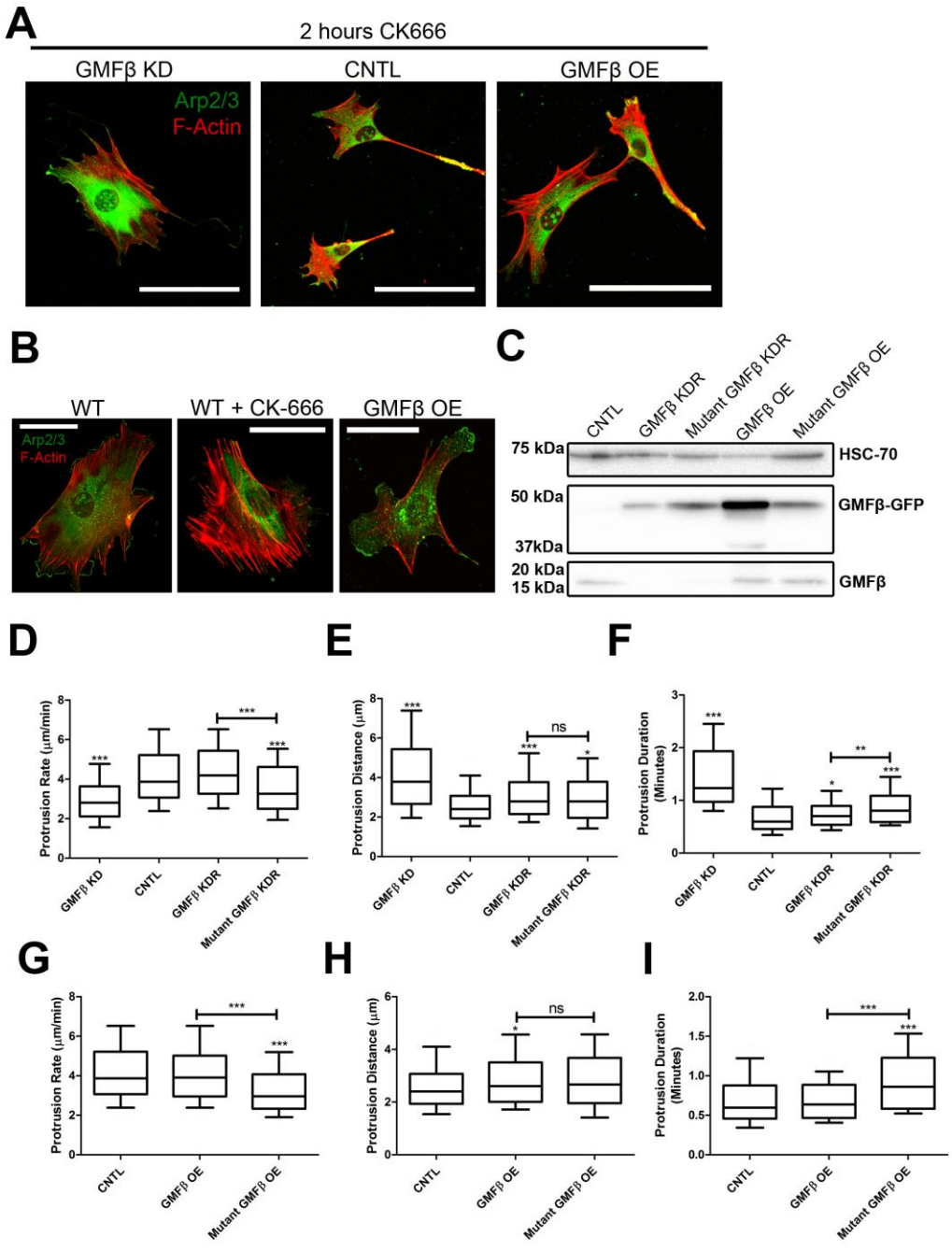

Supplemental Figure 2.2 A debranching deficient mutant of GMFβ cannot replicate GMFβ overexpression phenotypes or rescue GMFβ depletion, related to figure 4.

(A) Immunostaining of Arp2/3 (anti-p34) (green) and F-actin (red) in cells treated with CK-666 for two hours. 100μm scale bar.

(B) Immunostaining of Arp2/3 (anti-p34) and F-actin in WT cells with synchronized lamellipodia (left), cells treated with CK-666 for 10 minutes (center), and a GMFβ

overexpressing cell with synchronized lamellipodia (right). CK-666, which inhibits Arp2/3, creates a very distinct phenotype to that of overexpression of GMFβ. 50 μm scale bar.

(C) Western blot representing expression level of mutant GMFβ-GFP compared to WT GMFβ-GFP for various cell types. Expression of mutant GMFβ-GFP to the same levels at WT GMFβ-GFP OE made cells unhealthy and stalled their growth, so a moderate overexpression level was used.

(D) Protrusion rate in μm/min for GMFβ depleted cells rescued with mutant GMFβ-GFP, as quantified from kymography analysis.

(E) Protrusion distance in μm GMFβ depleted cells rescued with mutant GMFβ-GFP, as quantified from kymography analysis.

(F) Protrusion duration in minutes GMFβ depleted cells rescued with mutant GMFβ-GFP, as quantified from kymography analysis.

(G) Protrusion rate in μm/min for mutant GMFβ overexpressing cells, as quantified from kymography analysis.

(H) Protrusion distance in μm for mutant GMFβ overexpressing cells, as quantified from kymography analysis.

(I) Protrusion duration in minutes for mutant GMFβ overexpressing cells, as quantified from kymography analysis.

For all graphs, error bars represent 10th-90th percentile. Kruskal-Wallis multiple comparison testing was performed, and significance was measured by Dunn's post-test. ($p<0.001$ = ***, $p < 0.01$ = **, $p <0.05$ = *)

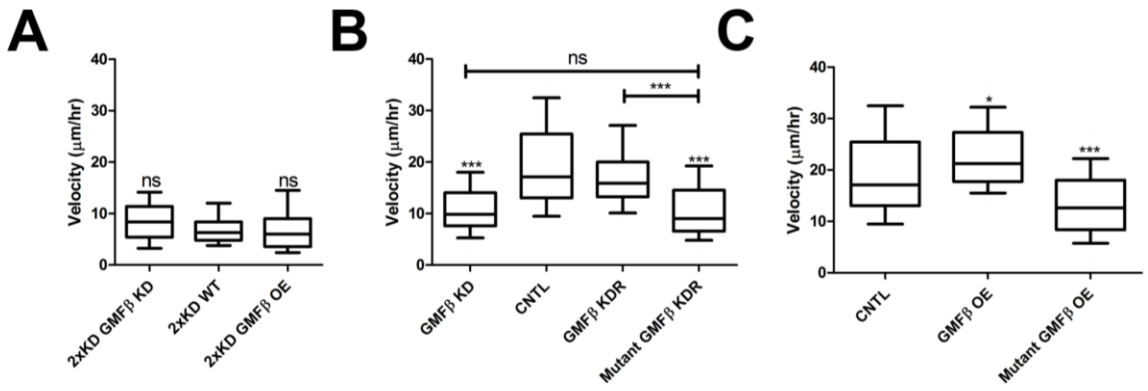

Supplemental Figure 2.3 Cell velocity in cells depleted of Arp2/3 and mutant GMFβ expressing cells, related to figure 5.

(A) Single cell velocity was measured for randomly migrating cells depleted of 2 subunits of Arp2/3 (2xKD). GMFβ overexpression or depletion had no significant effect on cell velocity in the absence of Arp2/3. KD N = 43, WT N = 42, OE N = 52.

(B) Single cell velocity of cells depleted of WT GMFβ and rescued with mutant GMFβ randomly migrating. GMFβ KD N = 70, CNTL N = 64, GMFβ KDR N = 77, mutant GMFβ KDR N = 98.

(C) Single cell velocity of mutant GMFβ overexpressing cells randomly migration. CNTL N = 70, GMFβ OE N = 74, mutant GMFβ OE N = 95.

For all graphs, error bars represent 10th-90th percentile. Kruskal-Wallis multiple comparison testing was performed, and significance was measured by Dunn's post-test. ($p<0.001$ = ***, $p < 0.01$ = **, $p <0.05$ = *)

CHAPTER THREE: DISCUSSION AND FUTURE WORK

Introduction

GMF is a highly conserved protein, found in simple eukaryotes like yeast as well as complex mammals like humans. The evolution of a protein that *specifically* acts upon Arp2/3 underscores the importance of Arp2/3 and branched actin in the cell, which are still being explored. Until recently, it was believed that cell lines devoid of Arp2/3 could not be generated. The generation of conditional knockouts of Arp2/3 subunits, as well as Ink4a/Arf$^{-/-}$ fibroblasts have led to great advances in our understanding of what Arp2/3 is obligatory for.

Understanding fully the importance of Arp2/3 is necessary to grasp all the reasons why GMF is important. However, there are many open questions about GMF that can be addressed in the near future. Broadly, these questions can be categorized into 1) GMF's biological role, 2) GMF's interacting proteins, and 3) the regulation of GMF.

What is GMF's Biological Role?

As previously introduced, global Arp2/3 depletion in most organisms is lethal. It is only recently that tissue specific and conditional knockouts have made studying the absence of Arp2/3 in physiological processes feasible, and may allow us to make new discoveries about the functions of Arp2/3 and branched actin (Zhou et al., 2013; Kim et al., 2013; Rotty et al.). However, knockout of Arp2/3 itself is very severe and disruptive to cellular and tissue architecture. More subtle perturbations to cellular branched actin content have the potential

to tell us a more nuanced story about Arp2/3. This is where perturbing GMF in animals becomes potentially quite interesting. Modulating GMF expression can act like the "volume dial" on branched actin in the cell. Depletion of GMF in different tissues or in an entire animal can reveal which populations of branched actin need to be more dynamic and more responsive, and which populations can tolerate the loss of a turnover mechanism.

Very limited work has been done on the knockout or knockdown of GMF in animals. No double knockdown or knockout of GMFβ and GMFγ has been performed in animals that have both isoforms. Knockdown of GMFγ has been shown to have severe phenotypes in angiogenic sprouting in microvascular endothelium, and GMFβ knockout mice have been shown to have defects in motor skills and learning (Lim et al., 2004; Zuo et al., 2013). No gross anatomical defects were reported in GMFβ knockout mice, but it should be noted that this group does not appear to acknowledge GMF as a cytoskeletal protein as of this date. Therefore, defects may go undetected because they did not predict effects outside of the brain and nervous system.

It is undetermined whether, physiologically, the two distinctly expressed isoforms of GMF can compensate for each other. Comparing individual knockout or knockdown phenotypes to a double knockout or knockdown would be a worthwhile venture. Likewise, rescuing a leukocyte or vascular GMFγ knockout with GMFβ may highlight any functional differences between the two isoforms.

The question of GMF's interaction with other actin disassembly proteins such as cofilin, coronin, and AIP1, as well as its potential competition with NPFs would make other combinations of double knockdowns attractive as well. As previously mentioned, *Drosophila* GMF depletion did not have particularly severe phenotypes until AIP1 was also depleted

(Poukkula et al., 2014). Dissecting the network of GMF's interacting proteins is a daunting prospect, but important to understanding the physiological significance of individual actin disassembly proteins.

What Other Proteins Functionally or Directly Interact with GMF?

There are several putative proteins which may directly or functionally interact with GMF. These include other actin disassembly proteins (cofilin, coronin, AIP1) and NPFs. Five separate groups have now explored GMF's effects on nucleation inhibition (Nakano et al., 2010; Gandhi et al., 2010; Boczkowska et al., 2013; Luan and Nolen, 2013). Our work has concluded that GMF's debranching function is more physiologically important than its potential antagonism of Arp2/3 activation, agreeing with Boczkowska et al. However, it is very difficult to separate debranching from nucleation inhibition functionally, and GMF's potential for NPF competition may play a more nuanced role in branched actin regulation.

The question of whether branches can be protected from GMF activity is also a relevant one. The type II NPF cortactin is known to stabilize Arp2/3 branches. It is possible that through cortactin's interaction with Arp2/3, it also serves as protection from disassembly by GMF. This could be addressed quite simply through *in vitro* actin polymerization studies, and *in vitro* TIRF. Genetic perturbation of cortactin could potentially enhance or rescue GMF knockdown/overexpression phenotypes.

Depletion of the cofilin enhancing protein AIP1 functionally synergizes to enhance GMF knockout phenotypes in *Drosophila* (Poukkula et al., 2014). It is unclear whether this is through perturbing cofilin mediated disassembly on top of GMF debranching, or a direct interaction. Since GMF is so closely related to cofilin, direct enhancement of GMF function by AIP1 is not entirely unlikely. Further research into this relationship is necessary.

In the initial biochemical characterization of GMF as a debrancher, coronin was shown to co-immunoprecipitate with GMF (Gandhi et al., 2010). No further characterization of this interaction has been completed. Coronin1B itself is thought to debranch actin by replacing Arp2/3 at the branch junction (Cai et al., 2008). It is possible that GMF binding could potentially accelerate this mechanism, or alternatively, that debranching by coronin is intentionally dis-similar to GMF debranching. Coronin1B requires multiple steps to debranch a filament: binding to Arp2/3 and actin, dissociation of Arp2/3 from the mother filament and daughter filament, and destabilization of the branch resulting in disassembly. The kinetics of this process are not well defined, however it would make sense that this process would occur more slowly than debranching by GMF, which only requires two steps (binding and destabilization). Cofilin, coronin, and GMF may be differentially recruited to branched actin depending on the kinetic, steric, and temporal requirements of the system.

Do Different Disassembly Proteins Have Distinct Roles?

A curious observation from the data presented here is that upon addition of CK-666, there is an initial drop in Arp2/3 signal common to WT and GMFβ depleted cells (a GMF-insensitive Arp2/3 population). There is then a portion of branched actin signal that dwells for longer in GMFβ depleted cells (a GMF-sensitive Arp2/3 population). What is the difference between these two populations of Arp2/3?

Two explanations exist: there is a population of Arp2/3 associated with NPFs at the membrane which dissociates upon CK-666 binding. It has not yet been characterized whether CK-666 can bind to NPF associated Arp2/3, though Arp2/3 in branches is inaccessible to CK-666. Alternately, the drop in signal may represent the action of other forms of F-actin

disassembly by proteins like cofilin and coronin. The true answer is likely a combination of both of these hypotheses.

Therefore, the initial drop in Arp2/3 signal provides a window to look at the contribution of cofilin, coronins, and other actin disassembly proteins to branched actin turnover in the lamellipodia. Modulating the activity of cofilin or coronins through drugs or genetic manipulation may change how quickly an initial loss of Arp2/3 signal occurs, or even rescue the delayed Arp2/3 turnover in absence of GMF. This can inform us of how strongly a protein is contributing the lamellipodial branched actin disassembly.

The generation of barbed ends is likely a key difference in the choice to debranch or to sever actin. If a branch is severed, there still exists a barbed end for new actin polymerization. Debranching does not generate a new barbed end, and leads to dissociation of Arp2/3 from the mother filament in the case of coronin1B. It is unclear whether Arp2/3 dissociates from the mother filament during GMF mediated disassembly. If it does not, a new branch may be able to be nucleated from the still-bound Arp2/3 after GMF debranching. Coronin1B mediated debranching would completely remove a branch from that vicinity. The subtle differences in management of actin creation could add up to physiologically relevant differences in how cells respond to their environment.

How is GMF Regulated?

Finally, there is the question of how GMF activity is regulated. Putative phosphorylation sites have been identified on serines 2 and 4, and tyrosine 104 of GMF (Ikeda et al., 2006; Ydenberg et al., 2013; Luan and Nolen, 2013; Wang et al., 2014; Boczkowska et al., 2013). Literature provides conflicting evidence on the importance of these phosphorylation sites. It was thought since the N-terminal serine is so important in

cofilin regulation, that GMF would be regulated similarly. So far, there is no compelling evidence that serine phosphorylation plays as large a role in GMF regulation as it does in cofilin. Yeast mutations of the tyrosine phosphorylation site were also not documented to have significant disruption in activity (Ydenberg et al., 2013). There are no kinases or phosphatases proven to act on the N-terminal serine sites, although phosphorylation was reported to be enhanced by cdc42 and Rac (Ikeda et al., 2006).

Though phosphorylation has been the subject of all current experiments regarding GMF's regulation (primary due to the assumption it would be regulated as cofilin is), other methods could be used to regulate GMF function. There is some evidence to suggest its transcriptional regulation through different stages of development (Zuo et al., 2013). GMF could be repressed or activated by interaction with a protein partner or protein complex. Interactions with other protein partners or complexes could also serve to either target GMF to a specific area, or sequester it away from a site of active branching. GMF could also be controlled through ubiquitination and other means of degradation. Little to no information exists supporting or excluding any of these possibilities.

Summary

GMF is a fascinating protein. Despite its small size of 17kda, it packs a punch in actin regulation. There remain so many basic questions to ask about GMF and its role in lamellipodial selection, retraction, and maintenance. Not only can we answer questions about GMF through these studies, but we can also answer very basic questions about lamellipodial behavior and the importance of Arp2/3 in cells and whole animals. I look forward to keeping an eye out for future research on GMF, and anticipate some exciting developments and resolutions to these basic questions.

REFERENCES

1. Boczkowska, M., G. Rebowski, and R. Dominguez. 2013. Glia maturation factor (GMF) interacts with Arp2/3 complex in a nucleotide state-dependent manner. *J Biol Chem*. 288:25683–25688. doi:C113.493338 [pii] 10.1074/jbc.C113.493338.

2. Cai, L., A.M. Makhov, D.A. Schafer, and J.E. Bear. 2008. Coronin 1B antagonizes Cortactin and remodels Arp2/3-containing actin branches in lamellipodia. *Cell*. 134:828–842. doi:10.1016/j.cell.2008.06.054.

3. Gandhi, M., B.A. Smith, M. Bovellan, V. Paavilainen, K. Daugherty-Clarke, J. Gelles, P. Lappalainen, and B.L. Goode. 2010. GMF is a cofilin homologue that binds Arp2/3 complex to stimulate filament debranching and inhibit actin nucleation. *Curr. Biol.* 20:861–867. doi:10.1016/j.cub.2010.03.026.

4. Ikeda, K., R.K. Kundu, S. Ikeda, M. Kobara, H. Matsubara, and T. Quertermous. 2006. Glia maturation factor-gamma is preferentially expressed in microvascular endothelial and inflammatory cells and modulates actin cytoskeleton reorganization. *Circ Res*. 99:424–433. doi:01.RES.0000237662.23539.0b [pii] 10.1161/01.RES.0000237662.23539.0b.

5. Kim, I.H., B. Racz, H. Wang, L. Burianek, R. Weinberg, R. Yasuda, W.C. Wetsel, and S.H. Soderling. 2013. Disruption of Arp2/3 results in asymmetric structural plasticity of dendritic spines and progressive synaptic and behavioral abnormalities. *J. Neurosci.* 33:6081–92. doi:10.1523/JNEUROSCI.0035-13.2013.

6. Lim, R., A. Zaheer, H. Khosravi, J.H. Freeman, H.E. Halverson, J.A. Wemmie, and B. Yang. 2004. Impaired motor performance and learning in glia maturation factor-knockout mice. *Brain Res.* 1024:225–232. doi:10.1016/j.brainres.2004.08.003.
7. Luan, Q., and B.J. Nolen. 2013. Structural basis for regulation of Arp2/3 complex by GMF. *Nat. Struct. Mol. Biol.* 20:1062–1068. doi:10.1038/nsmb.2628.

8. Nakano, K., H. Kuwayama, M. Kawasaki, O. Numata, and M. Takaine. 2010. GMF is an evolutionarily developed Adf/cofilin-super family protein involved in the Arp2/3 complex-mediated organization of the actin cytoskeleton. *Cytoskelet.* 67:373–382. doi:10.1002/cm.20451.

9. Poukkula, M., M. Hakala, N. Pentinmikko, M.O. Sweeney, S. Jansen, J. Mattila, V. Hietakangas, B.L. Goode, and P. Lappalainen. 2014. GMF Promotes Leading-Edge Dynamics and Collective Cell Migration In Vivo. *Curr Biol*. 24:2533–2540. doi:S0960-9822(14)01130-0 [pii] 10.1016/j.cub.2014.08.066.

10. Rotty, J.D., C. Wu, E.M. Haynes, C. Suarez, J.D. Winkelman, H.E. Johnson, J.M. Haugh, D.R. Kovar, and J.E. Bear. Profilin-1 Serves as a Gatekeeper for Actin Assembly by Arp2/3-Dependent and -Independent Pathways. *Dev. Cell*.

doi:http://dx.doi.org/10.1016/j.devcel.2014.10.026.

11. Wang, T., R.A. Cleary, R. Wang, and D.D. Tang. 2014. GMF-γ Phosphorylation at Tyr-104 Regulates Actin Dynamics and Contraction in Human Airway Smooth Muscle. *Am. J. Respir. Cell Mol. Biol.* doi:10.1165/rcmb.2014-0125OC.

12. Ydenberg, C.A., S.B. Padrick, M.O. Sweeney, M. Gandhi, O. Sokolova, and B.L. Goode. 2013. GMF severs actin-Arp2/3 complex branch junctions by a cofilin-like mechanism. *Curr. Biol.* 23:1037–1045. doi:10.1016/j.cub.2013.04.058.

13. Zhou, K., A. Muroyama, J. Underwood, R. Leylek, S. Ray, S.H. Soderling, and T. Lechler. 2013. Actin-related protein2/3 complex regulates tight junctions and terminal differentiation to promote epidermal barrier formation. *Proc. Natl. Acad. Sci. U. S. A.* 110:E3820–9. doi:10.1073/pnas.1308419110.

14. Zuo, P., Z. Fu, T. Tao, F. Ye, L. Chen, X. Wang, W. Lu, and X. Xie. 2013. The expression of glia maturation factors and the effect of glia maturation factor-gamma on angiogenic sprouting in zebrafish. *Exp Cell Res*. 319:707–717. doi:S0014-4827(13)00007-4 [pii] 10.1016/j.yexcr.2013.01.004.